$7

QEX

March/April 2018

www.arrl.org

A Forum for Communications Experimenters

Issue No. 307

KØZR designs a 20 meter band-pass filter for use at high power levels.

ARRL The national association for AMATEUR RADIO™
225 Main Street
Newington, CT USA 06111-1494

New

APRS® / D-STAR®

TH-D74A 144/220/430 MHz Tribander

Introducing the TH-D74A for the ultimate in APRS and D-STAR performance. KENWOOD has already garnered an enviable reputation with the TH-D72A handheld APRS amateur radio transceiver. And now it has raised the bar even further with the new TH-D74A, adding support for D-STAR, the digital voice & data protocol developed by the JARL, and enabling simultaneous APRS and D-STAR operation – an industry first.

- APRS compliance using packet communication to exchange real-time GPS position information and messages
- Compliant with digital/voice mode D-STAR digital amateur radio networks
- Built-in high performance GPS unit with Auto Clock Setting
- Wide-band and multi-mode reception
- 1.74” (240 x 180 pixel) Transflective color TFT display
- IF Filtering for improved SSB/CW/AM reception
- High performance DSP-based audio processing & voice recording
- Compliant with Bluetooth, microSD & Micro-USB standards
- External Decode function (PC Decode 12kHz IF Output, BW:15 kHz)
- Free software for Memory and Frequency Control Program
- Data Import / Export (Digital Repeater List, Call sign, Memory Channel)
- Four TX Power selections (5/2/0.5/0.05 W)
- Dust and Water resistant IP54/55 standards

APRS (The Automatic Packet Reporting System) is a registered American trademark of WB4APR (Mr. Bob Bruninga).
D-Star is a digital radio protocol developed by JARL (Japan Amateur Radio League).

KENWOOD

Customer Support/Distribution Customer Support:
(310) 639-4200 Fax: (310) 537-8235

www.kenwood.com/usa

JQA-1205 091
ISO9001 Registered
Professional Systems Business Group JVCKENWOOD Corporation

ADS#29016

QEX (ISSN: 0886-8093) is published bimonthly in January, March, May, July, September, and November by the American Radio Relay League, 225 Main Street, Newington, CT 06111-1494. Periodicals postage paid at Hartford, CT and at additional mailing offices.

POSTMASTER: Send address changes to: QEX, 225 Main St, Newington, CT 06111-1494
Issue No 307

Publisher
American Radio Relay League

Kazimierz "Kai" Siwiak, KE4PT
Editor

Lori Weinberg, KB1EIB
Assistant Editor

Zack Lau, W1VT
Ray Mack, W5IFS
Contributing Editors

Production Department

Steve Ford, WB8IMY
Publications Manager

Michelle Bloom, WB1ENT
Production Supervisor

Sue Fagan, KB1OKW
Graphic Design Supervisor

David Pingree, N1NAS
Senior Technical Illustrator

Brian Washing
Technical Illustrator

Advertising Information Contact:

Janet L. Rocco, W1JLR
Business Services
860-594-0203 – Direct
800-243-7768 – ARRL
860-594-4285 – Fax

Circulation Department

Cathy Stepina, *QEX Circulation*

Offices

225 Main St, Newington, CT 06111-1494 USA
Telephone: 860-594-0200
Fax: 860-594-0259 (24 hour direct line)
e-mail: **qex@arrl.org**

Subscription rate for 6 issues:

In the US: $29;

US by First Class Mail: $40;

International and Canada by Airmail: $35

Members are asked to include their membership control number or a label from their QST when applying.

In order to ensure prompt delivery, we ask that you periodically check the address information on your mailing label. If you find any inaccuracies, please contact the Circulation Department immediately. Thank you for your assistance.

About the Cover

Jeff Crawford, KØZR, describes some of the considerations essential to a successful design of a high-power filter. The 20 m example band-pass filter was designed to achieve a minimum of 50 dB stop band attenuation, while also taking advantage of the transmission zeros at 7 and 21 MHz.

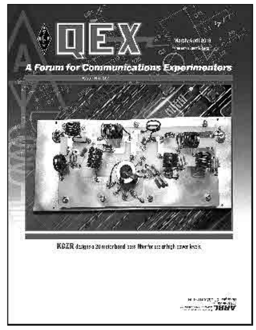

In This Issue

Features

Index of Advertisers

The American Radio Relay League

The American Radio Relay League, Inc, is a noncommercial association of radio amateurs, organized for the promotion of interest in Amateur Radio communication and experimentation, for the establishment of networks to provide communications in the event of disasters or other emergencies, for the advancement of the radio art and of the public welfare, for the representation of the radio amateur in legislative matters, and for the maintenance of fraternalism and a high standard of conduct.

ARRL is an incorporated association without capital stock chartered under the laws of the state of Connecticut, and is an exempt organization under Section 501(c)(3) of the Internal Revenue Code of 1986. Its affairs are governed by a Board of Directors, whose voting members are elected every three years by the general membership. The officers are elected or appointed by the Directors. The League is noncommercial, and no one who could gain financially from the shaping of its affairs is eligible for membership on its Board.

"Of, by, and for the radio amateur," ARRL numbers within its ranks the vast majority of active amateurs in the nation and has a proud history of achievement as the standard-bearer in amateur affairs.

A *bona fide* interest in Amateur Radio is the only essential qualification of membership; an Amateur Radio license is not a prerequisite, although full voting membership is granted only to licensed amateurs in the US.

Membership inquiries and general correspondence should be addressed to the administrative headquarters:

ARRL
225 Main Street
Newington, CT 06111 USA
Telephone: 860-594-0200
FAX: 860-594-0259 (24-hour direct line)

Officers

President: Rick Roderick, K5UR
PO Box 1463, Little Rock, AR 72203

Chief Executive Officer: Barry Shelly, N1VXY

The purpose of *QEX* is to:

1) provide a medium for the exchange of ideas and information among Amateur Radio experimenters,

2) document advanced technical work in the Amateur Radio field, and

3) support efforts to advance the state of the Amateur Radio art.

All correspondence concerning *QEX* should be addressed to the American Radio Relay League, 225 Main Street, Newington, CT 06111 USA. Envelopes containing manuscripts and letters for publication in *QEX* should be marked Editor, *QEX*.

Both theoretical and practical technical articles are welcomed. Manuscripts should be submitted in word-processor format, if possible. We can redraw any figures as long as their content is clear. Photos should be glossy, color or black-and-white prints of at least the size they are to appear in *QEX* or high-resolution digital images (300 dots per inch or higher at the printed size). Further information for authors can be found on the Web at **www.arrl.org/qex/** or by e-mail to **qex@arrl.org**.

Kazimierz "Kai" Siwiak, KE4PT

Perspectives

Diversity

Reactions to "Constraints" in the previous *QEX* were gratifying. "Just like with antennas, article diversity is a strength, not a weakness!" writes *QEX* reader and author Jan Simons, PAØSIM. We concur. Larry Copeland, KB1UMD, writes in detail, and we quote.

"Regarding 'Perspectives' in *QEX* Jan./Feb. 2018, I greatly enjoy *QEX* and wish that it were twice as long! I devour it!.... I don't mind that some articles are over my head, they fire the imagination.... I most value *QEX* for its tutorial qualities. Leave articles about operation, DXpeditions, contest scores, society news, product reviews, FCC doings, and so on to *QST* and *CQ*. Those magazines can and should cover "simpler" construction and design articles. The day we stop publishing schematics, we are doomed...."

"We risk becoming a hobby of appliance operators with the dumbing down of technical skills.... [But] our communications skills...are still enormously valuable. Witness all the greatly appreciated volunteer ham emergency communications work during recent hurricanes. The hobby is also at great risk from HOAs and other station restrictions. The clever technically persistent ham can DX even under rather severe restrictions."

"I was a CW Novice in the 1960s (WN1KSR). But life got in the way.... and I lost years. Some excellent ham co-workers...discovered that I was once a ham and pounded on me to get back in, for which I am very grateful.... I was astounded by the new gear when I set up a modest station in 2010. Radios were small, dripping with features, filtering that we could only dream of, modes and bands, and they didn't drift!"

"I badly wanted to build *something* homebrew and was thrilled to make a serviceable antenna tuner from junk box parts.... Moon bounce, antenna simulation, Smith charts, mesh networks and digital modes fascinate me. Maintaining technical expertise in ham radio is crucial. There is a place for communications skills, store-bought gear, emergency preparedness and organization in ham radio. But the technical core of ham radio is vital — we need *QEX*!"

"Computer and signal processing expertise has given us digital modes, moon bounce, ham satellites, repeaters, EchoLink and other internet-connected VOIP facilities. Appliance operators did not invent these things."

"A suggestion: any worthy articles...that do not fit in *QEX*...ought to go on an ARRL website somewhere.... Such articles could trigger lively, healthy debate!.... You can add my vote for a bigger *QEX*."

In This Issue

Our *QEX* authors contributed to the communications experimental arts in diverse Amateur Radio topics.

Jeff Crawford, KØZR, designs kilowatt-level HF band-pass filters with bandwidths up to 5%.

Al Christman, K3LC, optimizes an 8-circle vertical array.

Rudy Severns, N6LF, studies insulated *vs.* bare copper wire for antenna radials.

Dan Bobczynski, KG4HNS, resistor search program dramatically increases your resistor inventory.

Chuck MacCluer, W8MQW, proposes a method of quadrature direction finding.

Keep the full-length *QEX* articles flowing in, but if brevity is your forte, share a brief **Technical Note** of perhaps several hundred words in length plus a figure or two. Expand on another author's work and add to the Amateur Radio *institutional memory* with your technical observation. Let us know that your submission is intended as a **Note**.

QEX is edited by Kazimierz "Kai" Siwiak, KE4PT, (**ksiwiak@arrl.org**) and is published bimonthly. *QEX* is a forum for the free exchange of ideas among communications experimenters. The content is driven by you, the reader and prospective author. The subscription rate (6 issues per year in the United States is $29. First Class delivery in the US is available at an annual rate of $40. For international subscribers, including those in Canada and Mexico, *QEX* can be delivered by airmail for $35 annually. Subscribe today at **www.arrl.org/qex**.

Would you like to write for *QEX*? We pay $50 per published page for articles and Technical Notes. Get more information and an Author Guide at **www.arrl.org/qex-author-guide**. If you prefer postal mail, send a business-size self-addressed, stamped (US postage) envelope to: *QEX* Author Guide, c/o Maty Weinberg, ARRL, 225 Main St, Newington, CT 06111.

Very best regards,

Kazimierz "Kai" Siwiak, KE4PT

Jeff Crawford, KØZR

19735 Lovella Country Ct., Purcellville, VA 20132; **k0zr@ieee.org**

High-Power HF Band-Pass Filter Design

K0ZR covers some of the considerations essential to a successful high-power filter design in an example 20 m band pass filter.

The first step in a filter design for high power and contesting applications, in my opinion, is to leave nothing to chance or hope. At the 1,500 watt level there is little room for mistakes.

Let's consider a filter with a dissipative insertion loss of 0.3 dB. Simple mathematics shows that 100 W of that 1,500 W, will be dissipated in the filter. This heat will age the components more rapidly, may shift the filter's return loss as a function of duty cycle, and may unnecessarily cause thermal stresses to the filter, leading to possible premature failure. Heat is one of the enemies in high power filter design. The filter described here has about 0.1 dB insertion loss.

As a first step, one can carefully design a filter, paying special attention to notch placement for the adjacent contest bands, achieve acceptably low insertion loss, great return loss, thus reaching the point it is ready to build. This is only the first step. Consider the filter in Figure 1, which was designed with the "*q k*" method[1, 2]. Its response is shown in Figure 2. It has a rather clean passband, good return loss, and a smaller parts count than a comparable $N = 5$ elliptic filter. We discover, however, that at 1,500 W, some RF currents exceed a peak value of 100 A. I do not believe your printed circuit board will handle that current.

This example shows us that we need to consider alternate filter layouts. Knowledge of voltages, currents, parts values, core flux densities, and so on, are needed to avoid a possibly costly mishap. The intent over these next pages is to cover some of the considerations essential to a successful high-power design, rather than a complete design of a 20 m band pass filter. There are a considerable number of design references available, some of which we will reference here to facilitate your design efforts.

Getting Ready

A certain minimum tool set is necessary to successfully design a filter. A filter design package such as *Elsie*[3] is invaluable, and is available for free. A more traditional manual approach[4] is possible as well. A circuit simulation program such as *LTspice*[5] or *SIMetrix*[6] is essential for performing design tradeoffs, especially in ascertaining expected

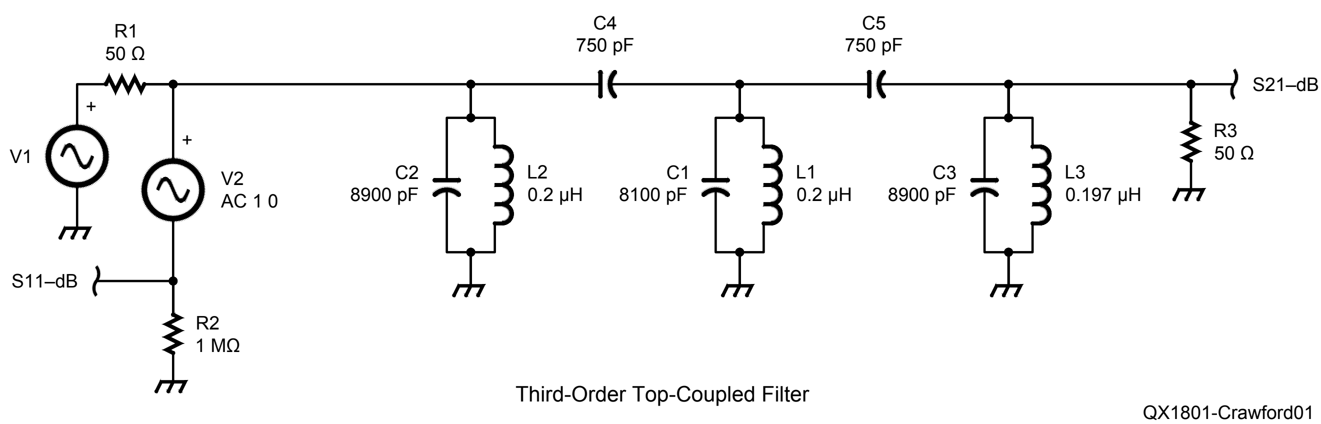

Figure 1 — Top-coupled filter.

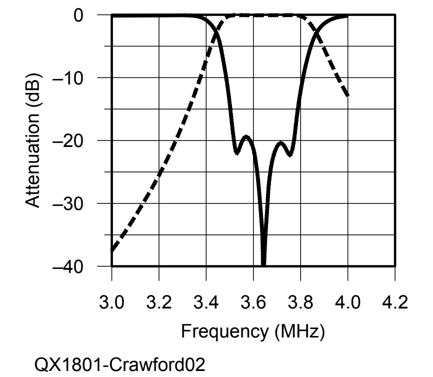

Figure 2 — Response of the filter in Figure 1.

operational voltages and currents. Test equipment to measure S_{21} and S_{11} is essential as well. Some short-cut methods can be used on simpler filter designs, however the filter of the complexity described here does not lend itself well to such an approach.

Discussion

The fundamentals covered here include filter loss, associated voltages and currents, and different design concepts such as impedance scaling of the filter, and use of powerful transform techniques, the Norton Transform in particular.

Minimizing Loss

As you delve deeper into general filter theory, you will encounter what are termed "elemental *g*-values" for Butterworth and Chebyshev filters. These "*g*-values", upon impedance and frequency scaling, evolve directly into the L and C values composing a low pass filter. The low pass filter can then be transformed into a band pass filter by resonating capacitors with inductors, and inductors with capacitors. There are multiple resources that describe how this is accomplished, some of which are cited[7, 8, 9] herein.

Your intuition may lead you to believe that the smaller the number of filter components, the lower the loss. This is not necessarily true. It can be shown theoretically that,

$$L = \frac{4.34}{wQ}\sum_i g_i \quad \text{where } w = \frac{\omega_2 - \omega_1}{\omega_o} \qquad (1)$$

L is the filter loss,

Q is the unloaded Q of resonators.

There are cases where a more complex filter, with higher filter order, actually has lower insertion loss than a simpler filter. It comes down to the calculated *g*-values for each implementation per Equation (1).

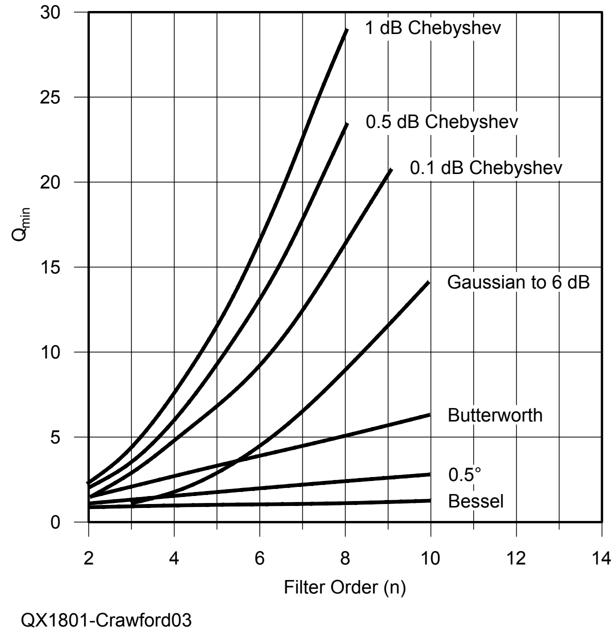

Figure 3 — Minimum *Q*s required in low pass filters.

Table 1
RF currents for 1,500 W and 50 Ω.

Component	*Amps*	*Component*	*Amps*	*Component*	*Amps*
L1	8.4	L5	6.7	C1	11.8
C5	6.7	L2	11.8	L6	20.6
C2	3.4	C6	9.6	L3	4.6
L7	2.7	C3	1.3	C7	7.8
L4	3.0	L8	4.5	C4	14
C8	12.5	L9	6.7	C9	4.5

Another important aspect of the design critical to loss is Q_{BP}, the Q of the pass band. In the case of the 20 m filter described here, ω_2 and ω_1 when multiplied by 2π, are 15.75 and 10.75 MHz, respectively, with a center frequency of 13.25 MHz. Q_{BP} is then,

$$Q_{BP} = \frac{13.25}{15.75 - 10.75} = 2.65 \qquad (2)$$

Any given low-pass filter has minimum Q-values that each L and C must exceed to attain the desired passband shape, see Figure 3-8 in Williams[10]. For band pass filters, these minimum Q values are multiplied by Q_{BP}. Had the designer of this filter opted for a narrow passband, such as 13 to 15 MHz, Q_{BP} would have been ~7 making the inductors that much more difficult, if not physically impossible to build see Equation (3).

$$Q = Q_{LP\ Minimum} \times Q_{BP} \qquad (3)$$

Q_{BP} in the 20 m case is made as low as possible to offset this effect while still attaining the desired rejection at 7 MHz and 21 MHz. Additionally, heightened Qs in resonators[11] will impact the accompanying voltages and currents, possibly further complicating your design and component selection. The needed Q is given in Equation (3).

If the low pass minimum required Q were 25 for example, the inductor Q would have to be higher,

$$Q = 25 \times 7 = 175 \qquad (4)$$

This example shows why band pass filter component selection can be more difficult than for low pass or high pass filters because of the Q_{BP} multiplying effect. Figure 3 illustrates the increasing minimum Q of low pass elements as the filter order increases, with filter family as a parameter. The Q_{BP} impact is precisely why the passband for the 20 m filter is a full 5-MHz wide even though the 20 m band is 350 kHz in width.

Other Factors in Loss

A familiar and often used expression for air-core coil inductance is,

Table 2
RF voltage at 1,500 W input.

Load, •	*L3, V*	*L5, V*	*C5, V*	*L7, V*
25	510	220	850	390
50	485	270	1,100	400
75	520	320	1,300	430
100	560	360	1,430	460
100 at 2 kW	645	-	1,600	-

$$L = \frac{r^2 n^2}{9r + 10s}$$

where r is radius in inches, n is the number of turns and s is the coil length.

This is just a starting point and can be rather inaccurate as the length to diameter aspect ratio changes, frequency increases, and wire size is varied. There is an optimum range of coil aspect ratios which, when chosen, will heighten the available Q of the coils. An internet-based tool[12] employed in this design uses modified Bessel functions for wire loss, and considers the length of the coil as a function of wavelength at the frequency of operation. The coils used in the subject design have a diameter of 0.75 inches and theoretical Qs of approximately 400.

Voltages and Currents

The opening example (Figure 1) served to emphasize the all-important consideration of voltages and currents encountered in a filter. The best means to assess these conditions is through use of the circuit analysis tools previously mentioned. They are valuable for "what if analyses", such as, "what happens to my RF currents if the VSWR were to be 2:1 instead of a nice, perfect 1:1?" Table 1 shows RF currents and Table 2 shows the RF voltage that result from this analysis for the 20 m filter shown in the schematic of Figure 4.

At different power levels the currents are,

$$I_{Pow\,Lev} = I_{1500\,\mathrm{W}} \sqrt{\frac{Power}{1500}}$$

For different load conditions, simulations show approximately,

$$I_{25\,\Omega} = I_{50\,\Omega} \times 1.3$$
$$I_{100\Omega} = I_{50\Omega} \times 0.70$$

In constructing of this filter, capacitors are placed in series when higher breakdown voltages are required, and similarly, capacitors are placed in parallel to increase the net current capacity of a given capacitor. These capacitor combinations are annotated in Figure 4. Research revealed that CDV-16 capacitors can handle 5 A continuous current at HF. This serves as a guideline.

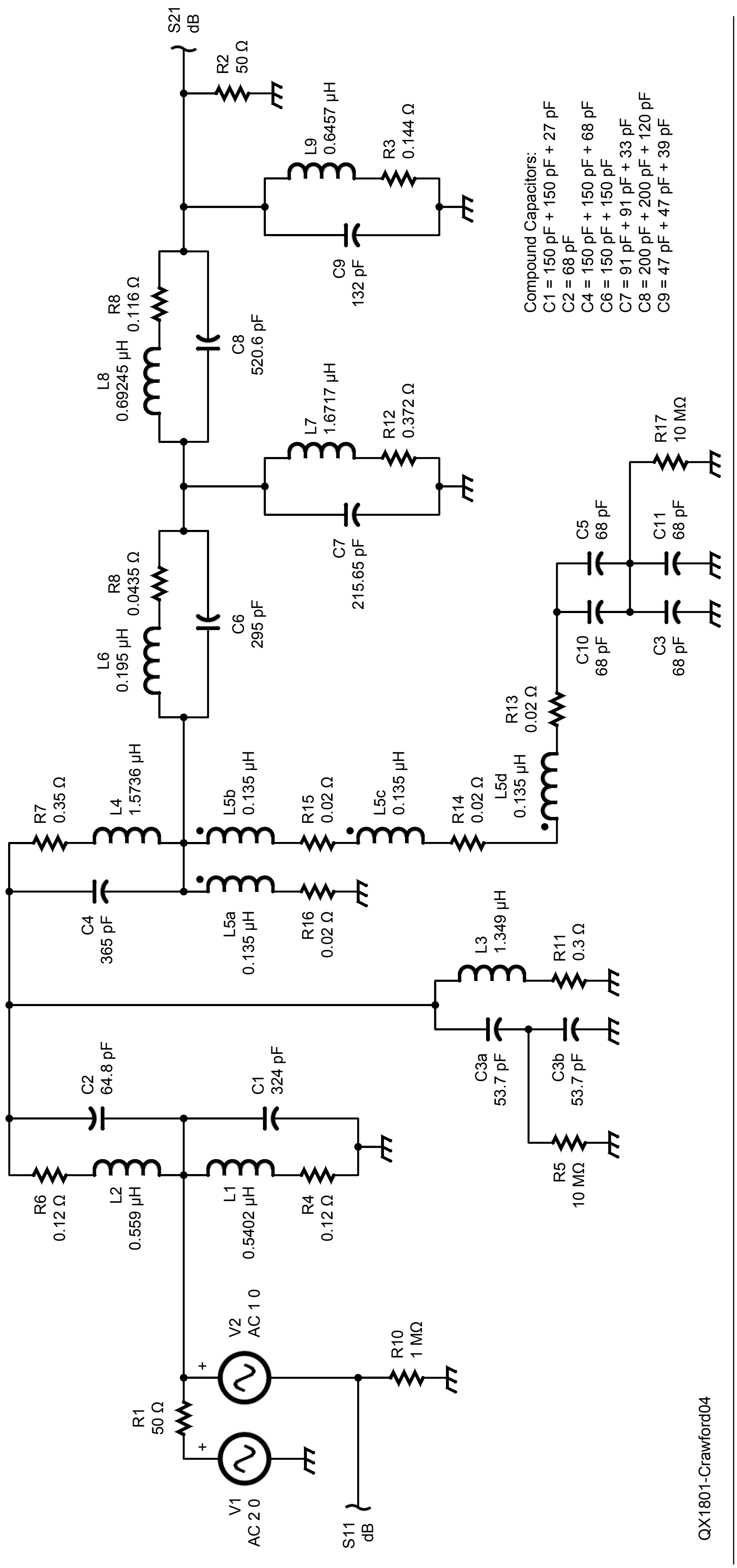

Figure 4 — Completed schematic for 20 m band pass filter.

Improving Filter Realizability and Performance

Although Figure 4 is the schematic of the filter as constructed, it began with the *Elsie* based schematic shown in Figure 5. There is quite a difference. A *SIMetrix* evaluation of Figure 5 revealed excessively high currents — more than 25 A — in resonator 4, the 178.7 nH inductor and 807 pF capacitor. There are some techniques that can be used to attack this problem. The first has already been employed by widening the passband to 5 MHz, and thus reducing Q_{BP}. This filter was designed around an impedance of 50 Ω. What if we designed it at 100 Ω and used impedance transformers at the input and output? This is an available option, but not selected for the following reasons.

Resonator 3 becomes large, elevating concerns about self-resonance in important parts of the stop band. Capacitor C2 takes on decreasing values making the idea of paralleling multiple capacitors troublesome. Simple *L*-networks at the input and output do not have sufficient bandwidth to comfortably handle 5 MHz. Other techniques could ameliorate this issue, but were not elected here.

We identified the use of Norton Transforms, and their use is now briefly outlined. Several references[13] go into greater detail for the interested reader. Norton transformations appear in several forms and are shown in the Table of Figure A. These transformations allow different capacitor and inductor arrangements to be replaced equivalently with a different capacitor and inductor arrangement accompanied by an ideal transformer. Through use of a 1:n Norton transformation near the input of the filter and a n:1 complimentary Norton transformation near the filter output, an impedance transformation can be inserted almost anywhere within the filter. The wide bandwidth characteristics of the ideal transformers are retained, as is not the case for an *L*-network matching implementation where filter impedance scaling is used.

The Table of Figure A addresses both capacitors and inductors. In the case of a series capacitor, row one of the Table, the equivalency using the pi-pad connected capacitors and ideal transformer is used. Had the series inductor been used, the pi-pad of inductors and ideal transformer would be used. These transforms are rather simply derived from cascaded *ABCD* matrices for the two circuits we wish to equate, and the relationships derived.

It bears repeating that this equivalency of the Norton transform technique is superior over bandwidth to a narrow-band solution of an input and output *L*-network. As the filter's center frequency increases, *L*-networks can

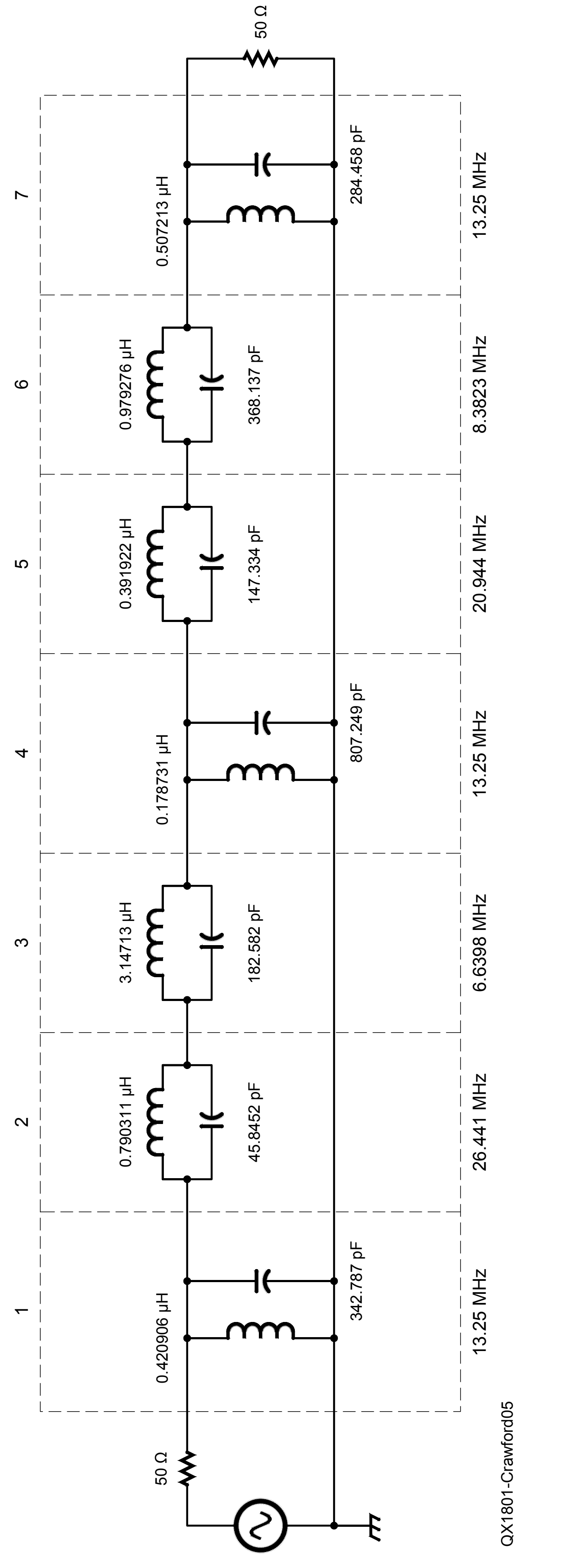

Figure 5 — A 5-th order elliptic filter designed using *Elsie*.

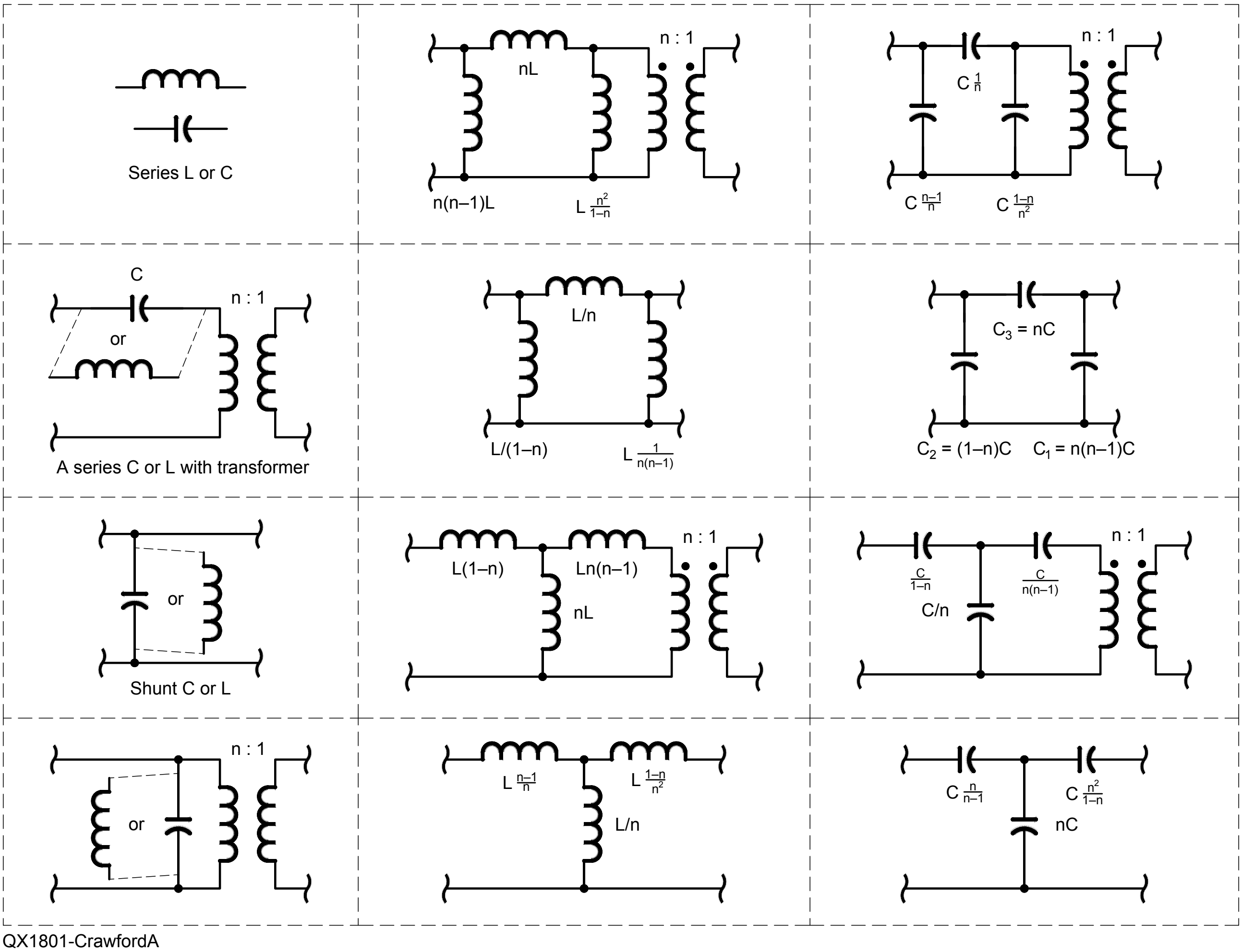

Figure A — Table of multiple Norton Transforms.

be utilized with more success, not being relegated to only capacitor networks — which for 1500 W run up costs — and the Norton Transform.

An additional Norton Transform[14], and the one used in this design, is that shown in Figure 6. This transform allows for an impedance step-up or step-down for a parallel *LC* network with an ideal capacitor.

Capacitors C_1, C_2, and C_3 in Figure 6 are derived from the simple algebraic expressions in the row-2 column-3 entry of the Figure A Table. The "*n*" is the transformer turns ratio.

There is a catch to the Norton approach, however. Upon study of the relationships in the Table of Figure A, one finds that there are always some resulting negative valued components. Consequently, when using the Norton technique, other components must be present to absorb these negative valued *L*s and *C*s. One of the intermediate steps in the 20 m filter design is shown in Figure 7 where, indeed, there are negative component values. Figures 8 and 9 show that these negative values are handled in the same manner traditional inductors and capacitors are combined.

The route to the final 20 m band pass filter design employed the Norton technique two times at two different locations within the filter. The first was required to alleviate the negative components that would result from the second transformation. The extra *L*s and *C*s in Figure 4 arise from the Norton Transform application. The two additional *LC* resonators (a) eliminate concerns about the otherwise floating node at this point, and (b) help equalize component values while

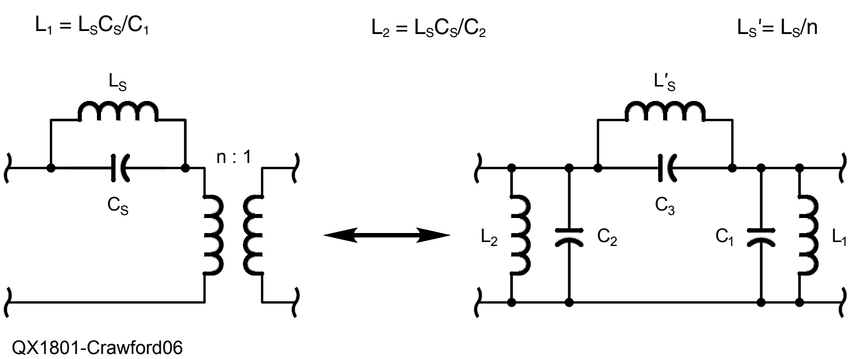

Figure 6 — An additional Norton Transform used in this design.

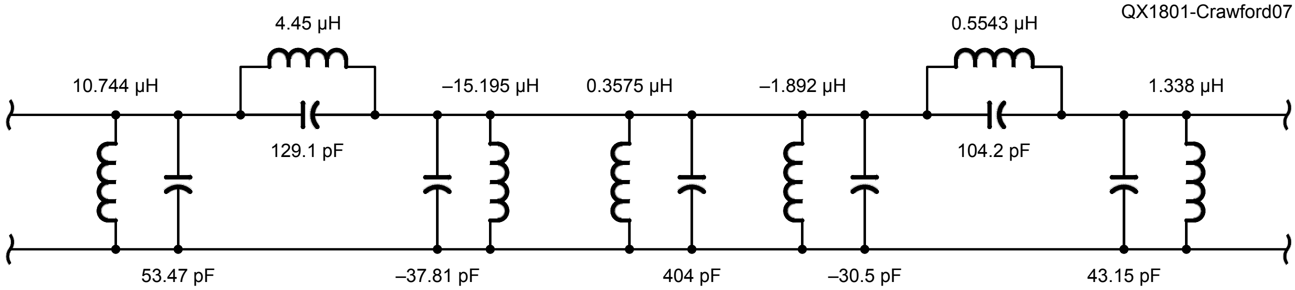

Figure 7 — One of the intermediate steps in the 20 m filter design is shown. Figures 8 and 9 show that these negative values are handled in the same manner traditional inductors and capacitors are combined.

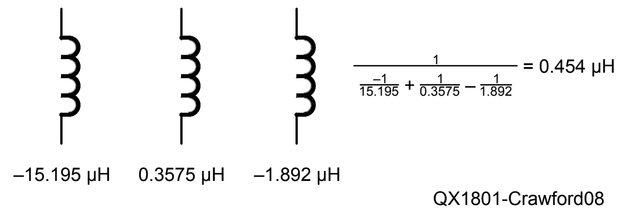

Figure 8 — Combining inductors that have negative values.

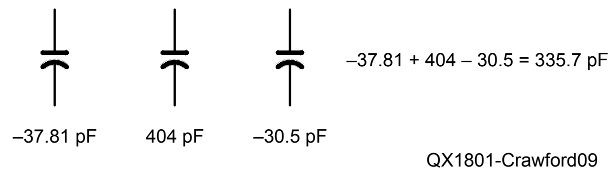

Figure 9 — Combining capacitors that have negative values.

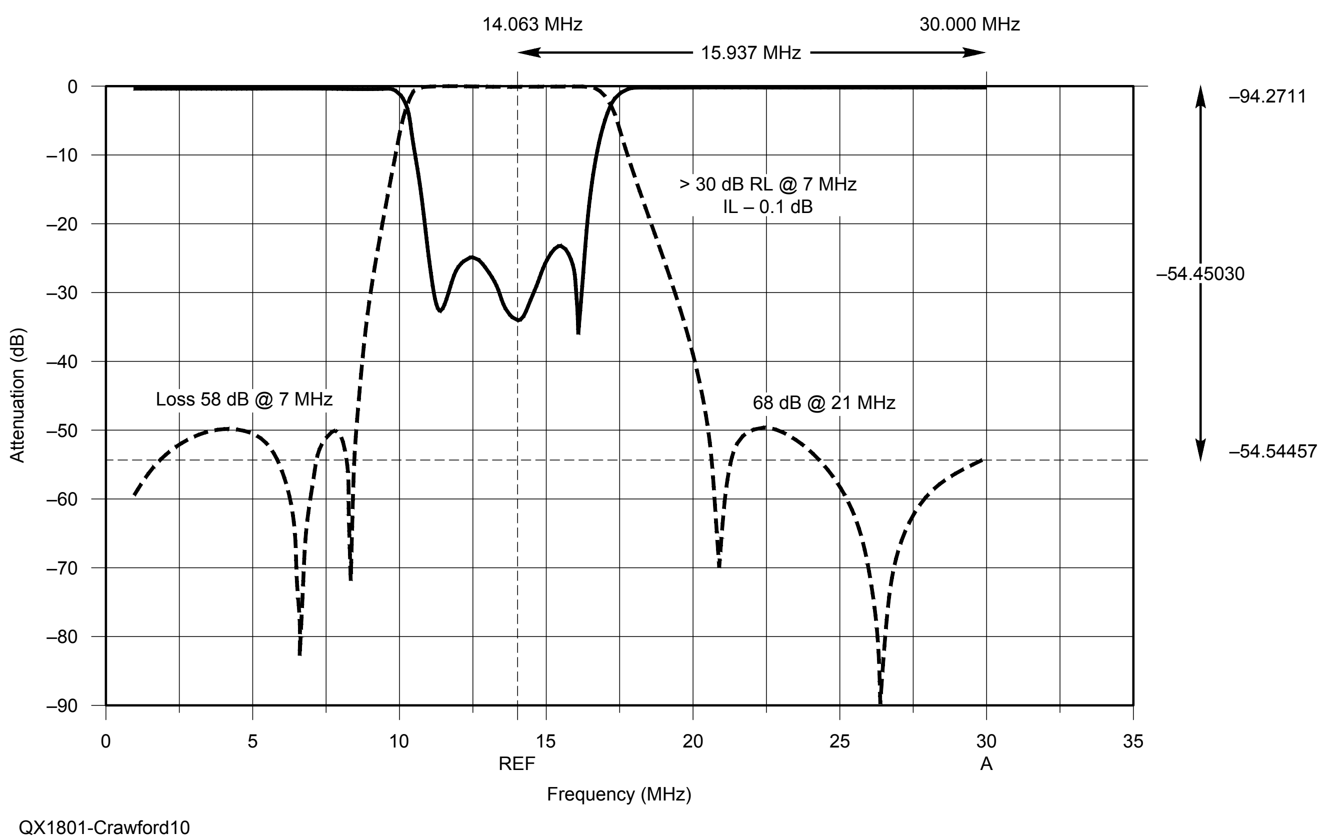

Figure 10 — Filter performance of the circuit in Figure 4 simulated with *SIMetrix*.

also diminishing currents and voltages in many cases. An in-depth discussion of the steps taken in the design is available at **www.k0zr.com**.

A Toroidal Transformer Solution

Techniques of optimizing inductor Qs, diminishing Q_{BP}, impedance scaling the filter directly, or manipulation through the use of Norton Transforms have been offered. There is yet another valuable technique presented to finalize the design. This technique is used throughout the low-power W3NQN filter designs[15].

While many good characteristics resulted from the Norton Transformation application, currents in the center resonator were considered too high. To reduce the current to more acceptable levels, the W3NQN technique of a multi-filar toroidal transformer is used. The prevailing voltages were sufficiently low such that core saturation was of no concern.

Further study of Figure 4 shows that a four-winding toroid ($L5a$, b, c, d) is used. The transformer is a quadrifilar transformer, four turns, making an impedance transformation of 16 times. The toroids are two stacked Amidon T-130-17cores. If one pulls apart this assembly of four coupled inductors, as shown in Figure 4, you see that indeed this is an autotransformer composed of the four different windings. Because there are four windings and the composite resonator is tapped just above the first one, an impedance change of 4^2 results, thus changing the inductor-capacitor currents from about 30 A to about 6.5 A. To maintain the same original LC resonant frequency, the factor of 16 multiplies the effective inductance so the accompanying capacitor must be reduced by a factor of 16. One additional consideration is that if the tap-point voltage were 270 V, the voltage on the resonating capacitor will be *four* times this value, or nearly 1.1 kV.

Figure 10 shows the filter performance, simulated by *SIMetrix*, of the circuit in Figure 4, and shown assembled in Figure 11. The insertion loss is theoretically about 0.1 dB, and the passband return loss for the 20 m band is better than 30 dB. Table 3 show a summary of the insertion loss and return loss of the filter. Figure 12 shows the S21 performance and Figure 13 shows the measured return loss.

Table 3
Insertion loss and return loss.

Frequency, MHz	*Insertion Loss, dB*	*Return Loss, dB*
3.5	~ 50	
7.0	65	
14.0	-	30
14.1	0.15	
14.35	-	28.4
21	58	
28	57	

The Filter Assembly

Figure 11 shows an image of the filter assembly. The board dimension are approximately 5.5 inches by 11 inches. The larger current-carrying inductors are wound with use #12 AWG thermaleze-coated wire. The several smaller inductors, including the toroid, use #14 AWG wire. All capacitors are CDV16s available through Mouser. These capacitors should safely handle 5 to 6 A each in the HF range. When needed, multiple values are placed in parallel for current sharing. Figure 14 is an image of the completed filter.

Filter Tuning

This filter topology lends itself nicely to final tuning. Each parallel LC resonator frequency can be easily found using,

$$f_0 = \frac{1}{2\pi\sqrt{LC}} .$$

The resonators with resonant frequencies

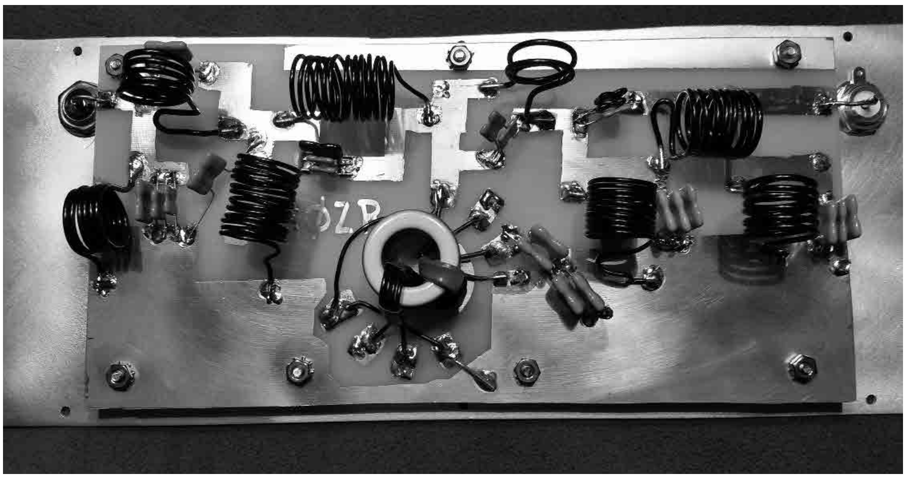

Figure 11 — The filter assembly. [Jeff Crawford, KØZR, photo]

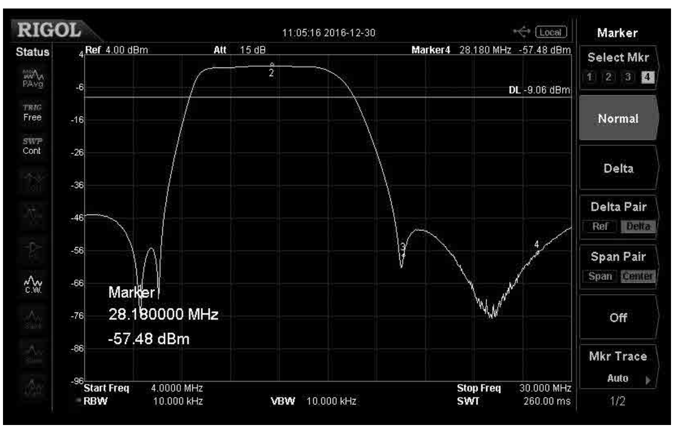

Figure 12 — The S22 performance of the filter.

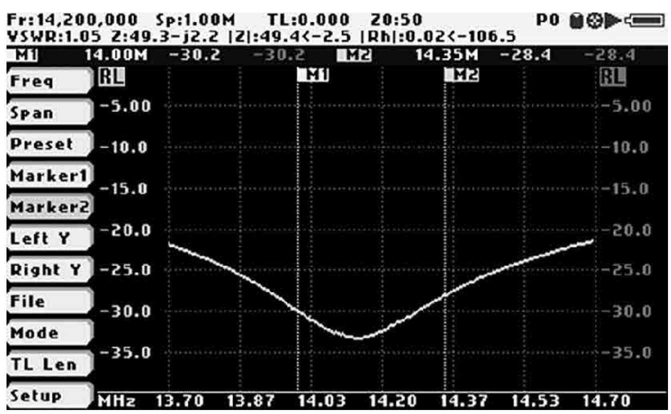

Figure 13 — Measured return loss of the filter.

Figure 14 — The completed 20 m band pass filter. [Jeff Crawford, KØZR, photo]

outside the passband form the deep notches in the stop bands. Those resonators are adjusted first, then the remaining resonators are adjusted to optimize passband return loss. It bears emphasizing the importance of tuning the filter pass band by optimizing return loss, *not* insertion loss.

Prior to assembly, each inductor was paralleled with a known capacitance and adjusted to what should be the resonant frequency for the "design-to" inductor value and known capacitor. This will save you many headaches in your assembly and tuning process.

Summary

The filter was designed to achieve a minimum of 50 dB stop band attenuation, while also taking advantage of the transmission zeros at 7 and 21 MHz. In operation at the 1500 W level, only inductors L_1 and L_2 were elevated in temperature, and only slightly, after ten minutes of constantly calling CQ. The cores were absolutely cold. The insertion loss is difficult to measure with the Rigol spectrum analyzer and tracking generator. The insertion loss appears to be about 0.1 dB. I will place a fan on the backside of the filter so as to lessen concerns about component heating. Component cost for this 20 m filter is approximately $100.

Jeff Crawford, KØZR, was licensed in 1969 at age 15 with the call sign WAØZRT. He upgraded to the Amateur Extra class in 1976, and adopted call sign KØZR. He earned a B.S. in Zoology from the University of Nebraska, in 1975, a BSEE from the University of Nebraska in 1983, and an MSEE from the University of Southern California in 1988. Jeff is a member of ARRL, Loudoun Amateur Radio Group, Potomac Valley Radio Club, and CWOPs, His first welding project was a 63 foot free-standing tower, still standing after almost 40 years. Jeff has designed and built assemblies to tip-over his crank-up tower, a base for a quarter-wave 80 m vertical, and a traveling hoist system in an out building. He enjoys design and analysis of RF and microwave systems. Jeff is an active contester in the larger world-wide contests. He has 304 DXCC entities confirmed on LOTW. Professionally, he is employed by a government think tank, specializing in RF and microwave hardware and systems.

Notes

[1] R. W. Rhea, *HF Filter Design and Computer Simulation*, McGraw-Hill, Inc., 1995.

[2] G. Matthaei, L. Young, and E. M. T. Jones, *Microwave Filters, Impedance-Matching Networks, and Coupling Structures*, Artech House, 1980.

[3] *Elsie* filter design and analysis, **www.tonnesoftware.com/elsie.html**.

[4] A. B. Williams, Electronic Filter Design Handbook, McGraw-Hill Book Company, 1981.

[5] *LTspice*, **www.linear.com/designtools/software/**.

[6] *SIMetrix*, **https://www.simetrix.co.uk/**.

[7] G. Matthaei, *et al.*, *op. cit.*

[8] R. W Rhea, *op.cit.*, pp. 169, 172, 174.

[9] J. Helszajn, *Synthesis of Lumped Element, Distributed and Planar Filters*, McGraw Hill, 1990.

[10] A. B. Williams, *op. cit.*

[11] W. H. Hayt and J. E. Kemmerly, *Engineering Circuit Analysis*, Chapters 13-14, McGraw-Hill Book Company, 1978.

[12] Single-Layer Helical Round Wire Coil Inductor Calculator, **hamwaves.com/antennas/inductance.html**.

[13] R. W Rhea, *op. cit.*, G. Matthaei, *et al.*, *op. cit.,* A. B. Williams, *op. cit.,* J. Helszajn, *op. cit.*

[14] A. Klappenberger, "Narrow Bandwidth Elliptic Bandpass Filters with Low Parts Value Spread," *RF Design*, Dec. 1992.

[15] W3NQN filters, **https://www.arraysolutions.com/w3nqn-filters-info**.

Al Christman, K3LC

Grove City College, 100 Campus Drive, Grove City, PA 16127-2104

A Study of 8-Circle Arrays

The 8-circle vertical array is compared to the 4-square phased-vertical array. Computer simulations indicate that an array designed for 75-meter SSB operation may also be used successfully on 80-meter CW.

Many hams use a 4-square phased-vertical antenna system for operation on the low bands, but those who are wishing for something more may have been wondering about the 8-circle array. Important questions which must be answered include "what spacing should I use?" and "what current phase-angles work best?" This article is an attempt to supply the information that is needed to answer those queries, and more.

The 8-circle array is usually constructed from 8 identical quarter-wave vertical monopoles that are equally-spaced around the perimeter of a large circle. Figure 1 shows the basic layout of the design. Any two adjacent elements, such as #4 and #5 in the figure, are configured to function as an end-fire array, as are the pair of adjacent elements which are located on the opposite side of the circle (#1 and #8). These two end-fire "sub-arrays" are then fed together in phase, to create a four-element broadside array which is shaped like a rectangle. The result is a "beam" which can be switched to fire in any of eight directions that are spaced 45 degrees apart in azimuth.

In our study of the 8-circle, we will assume that all of the feed-point current amplitudes are equal. Referring again to Figure 1, if elements 5 and 8 are fed with currents at 0° phase-angle, while elements 1 and 4 are fed with currents at some lagging phase-angle, then the main lobe of radiation will point directly toward the top of the page (North). The four inactive elements of the array have their bases open-circuited during normal operation, to render them electrically invisible.

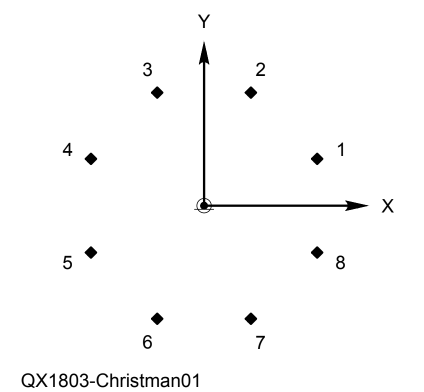

Figure 1 — Plan view of an 8-circle array, as generated by EZNEC. Eight identical quarter-wave vertical elements are placed at equal intervals around the perimeter of a circle. Only four monopoles are active at a time, while the four un-used elements are open-circuited at their feed-points. When firing directly North, monopoles #5 and #8 are driven with currents of 1 $\angle 0^\circ$ while the input currents to elements #1 and #4 are set at 1 $\angle \theta^\circ$, where the lag-angle θ is selected to achieve the desired performance characteristics. There are no radials in this model, since "MiniNEC" ground is employed here.

Parameter Variations

The antennas described here were simulated on the computer using the EZNEC software package[1]. For simplicity, each of the eight vertical monopoles in the array was modeled as an aluminum conductor which is 8" in diameter and 61.5 feet tall. These monopoles are resonant near 3790 kHz, when placed over "MiniNEC-style" ground with a conductivity of 0.005 Siemens/meter and a dielectric constant of 13.

Using the "MiniNEC" ground option allows the program to take the electrical characteristics of the soil into account when calculating both the gain of the antenna and the shape of the radiation pattern, see the "EZNEC reference manual". However, it also assumes that the ground is a perfect conductor when determining the impedance and current values. Neither ground rods nor a radial ground-screen are permitted with this type of model, so the computation time is relatively short. If the "High-Accuracy" ground option is selected, then some type of earth connection (such as ground rods or radials) must be included in the simulation. When in this mode, EZNEC utilizes a detailed "Sommerfeld-Norton" mathematical procedure to analyze the antenna, including its interaction with the ground system. If there are many radials in the design, then the calculation time can be much longer because of the added complexity of the model.

For our study, the radius of the circle on which the elements are placed is varied in one-foot increments between 70 and 90 feet. Similarly, the phase-angle of the base current applied to the front element ranges from -90 to -125 degrees, in steps of five degrees. This yields a total of 21 different computer models, and the data gathered from these simulations is displayed in Tables 1 through 21 respectively. Every table includes the following items: the phase-angle of the feed-point current in the front element of each end-fire pair; the peak forward gain, take-off angle, and front-to-back ratio in the elevation plane of the radiation pattern; the front-to-back ratio (or front-to-side ratio, whichever is lower) and half-power beamwidth in the azimuthal plane; and the resistive component of the input impedance of the back element in each end-fire pair.

Observations

A review of Tables 1 through 21 (at end of article) allows us to draw some general conclusions with regard to the performance of the array, when the circle radius and the current lag-angle are varied (at 3790 MHz):

- As the radius of the circle increases (with the phase-angles of the input currents kept constant) the peak forward gain of the antenna rises steadily (although the take-off angle where peak gain occurs also rises very slightly).
- As the radius of the circle increases, the front-to-back ratio (FBR) in the elevation plane rises steadily, as long as the phase-lag in the current drive to the front elements is between 90° and 105°. The elevation-plane FBR continually falls for current phase-lag angles of 120° and 125° as the circle's radius increases. For intermediate angles of phase-lag, the FBR in the elevation plane rises initially, but then eventually drops off.
- As the radius of the circle increases, the front-to-minor-lobe ratio in the azimuthal plane initially increases, but then decreases, for current phase-lag angles between 90° and 110°. For lag-angles from 115° and 125° the front-to-minor-lobe ratio continually decreases.
- As the radius of the circle increases, the input resistance of the back element in the end-fire pairs continually increases, ranging from a low of about 3.5 Ω to a high of roughly 9.8 Ω. At the same time, the input resistance of the front elements remains relatively high, within the range of 31 Ω to 45 Ω.
- Increasing the phase-lag of the current drive to the front elements (while the circle's radius remains fixed), will usually produce more forward gain, although that gain value will actually rise to a peak – and then decline very slightly – for those cases where the circle's radius is greater than 71 feet.
- If the radius of the circle is fixed, then the FBR in the elevation plane depends upon the amount of phase-lag applied to the drive currents for the front elements. The lag-angle which maximizes the FBR in the elevation-plane ranges from 115° when the radius of the circle is 70 feet, to 105° for a radius of 90 feet.
- If the radius of the circle is fixed, then the size of the undesirable minor lobes in the azimuthal plane is dependent upon the amount of phase-lag applied to the drive currents in the front elements. For most phase-lag angles, the side lobes are larger than the back lobe, but eventually the back lobe will begin to dominate when the phase-lag reaches about 110° to 115°. In general, the angle of phase-lag which produces the smallest minor lobes in the azimuthal plane is close to 110°, although this number may vary plus-or-minus five degrees for certain array sizes.
- If the radius of the circle is fixed, then the input resistance of the back elements [$R_{in(back)}$] depends upon the amount of phase-lag applied to the drive currents for the front elements. As the current lag-angle increases, the value of $R_{in(back)}$ initially decreases, but will eventually change direction and begin to get larger, as the phase-lag angle approaches its upper limit of 125°. The current phase-lag angle which yields the smallest value of input resistance is 120° if the circle's radius is 74 feet or less, and 115° for circles whose radius is larger than 74 feet.

Quadrature Feed

Some operators may prefer to utilize the classic quadrature-feed system for this array, with the back elements having base currents of 1 ∠0°, while currents of 1 ∠–90° are supplied to the front monopoles. Table 22 reveals the performance of the antenna under these input conditions, when the radius of the circle is varied between 70 and 90 feet. The peak forward gain of the array rises a bit each time the circle's radius is made larger, although the incremental improvement is minimal for radii beyond about 85 feet. In a similar fashion, the elevation-plane FBR also increases slightly as the circle gets bigger, although the improvement in FBR is small for radii greater than roughly 82 feet.

The story is different when we examine the secondary lobes in the azimuthal plane. Here, the back lobe is always smaller than any side lobes which may be present, for any circle radius from 70 to 90 feet. In other words, the FBR is always better (larger) than the front-to-side ratio (FSR) when using quadrature feed with this array, provided that the radius of the circle falls within the range of values given earlier. As the circle is made bigger, the FSR initially rises but then falls, reaching its maximum value when the circle's radius is equal to 81 feet.

Which Design is Best?

Choosing the "best" circle radius and the "best" current phase-lag angle for the two front elements depends upon the particular goals of the operator. For example, I decided that I wanted a design that yielded at least 18 dB of FBR in the elevation plane, along with at least 18 dB of FBR (or FSR) in the azimuthal plane. A review of the data tables (Tables 1 to 21) revealed that only a few of the many possible combinations of circle radius and phase-lag angle would meet my goal. These eleven options are listed in Table 23, where I have shown both the elevation-plane FBR and the azimuthal-plane FSR, as well as their average.

Scanning the list of choices, I decided that it would be good to have as much forward gain as possible, and – if feasible – maximize the input resistance at the terminals of the back elements. In general, the radiation efficiency of the antenna system is higher when the input resistances of the monopoles are larger. R_{in} for the front elements in these arrays is always above 30 Ω, so we don't need to worry about those. The last two entries in Table 23 both provide input-resistance values above 6 Ω, and their peak gains are similar. But, the larger array has less overall rejection of unwanted signals off the back and sides, and it takes up more space. Therefore, I will select a circle radius of 81 feet, with a phase-lag angle of 110° for the input current to the two front elements. With this radius, the spacing between the two monopoles in each end-fire sub-array is almost exactly 62 feet, while the distance between the two broadside pairs is equal to 149 feet 8 inches.

You have probably noticed that, throughout this analysis, I have changed the phase-angle of the drive current to the front elements in five-degree increments. At this point, it might be wise to "fine-tune" the design of the array by making one-degree adjustments in the lag-angle, and check to see if this might give us better performance. So, I kept the radius of the circle fixed at 81 feet, and varied the lag-angle of the front-element input current by plus-or-minus one degree, to see what would happen. The outcome is displayed in Table 24.

As it turns out, a phase-lag angle of 110° is actually the best choice for the currents which are applied to the two front elements of the antenna. Dropping the lag-angle to 109° yields a very small improvement in the value of R_{in} at the back elements, but it also reduces the forward gain of the array, as well the elevation-plane FBR. On the other hand, raising the lag-angle to 111° slightly reduces the value of R_{in} at the back elements, although the gain of the antenna remains unchanged. In addition, the FBR in the elevation plane and the FSR in the azimuthal plane both get smaller. The computer-generated plots for the elevation-plane and azimuthal-plane radiation patterns of the preferred array — circle radius = 81 feet, I_{front} = 1 ∠–110° and I_{back} = 1 ∠0° — are given in Figures 2 and 3 respectively.

The antenna design which I have selected as "the best" (described above) has a peak forward gain of 8.46 dBi at 23.3° take-off angle, and an elevation-plane FBR of 18.4 dB. A classic 4-square phased-vertical array, if constructed from the same type of monopoles and installed over the same "MiniNEC" ground, will generate 6.02 dBi

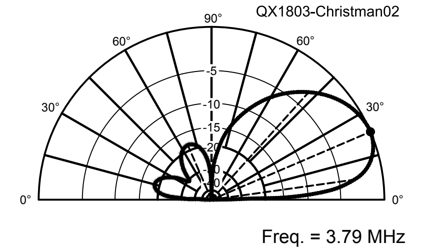

Figure 2 — Elevation-plane radiation pattern for the "best" 8-circle array design, when using "MiniNEC" ground. Circle radius is 81 feet, $I_{front} = 1 \angle -110°$ and $I_{back} = 1 \angle 0°$. Frequency is 3790 kHz, peak forward gain is 8.46 dBi at 23.3° take-off angle, front-to-back ratio is 18.4 dB, $Z_{in(front)} = 36.3 + j8.06\ \Omega$ and $Z_{in(back)} = 6.07 - j6.19\ \Omega$.

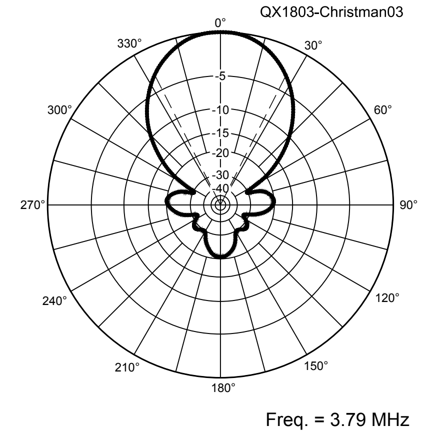

Figure 3 — Azimuth-plane radiation pattern for the "best" 8-circle array design, when using "MiniNEC" ground. Circle radius is 81 feet, $I_{front} = 1 \angle -110°$ and $I_{back} = 1 \angle 0°$. Frequency is 3790 kHz, front-to-back ratio is 20.1 dB at 23.3° take-off angle, front-to-side ratio is 20.2 dB at 23.3° take-off angle, half-power beamwidth is 53.2° at 23.3° take-off angle.

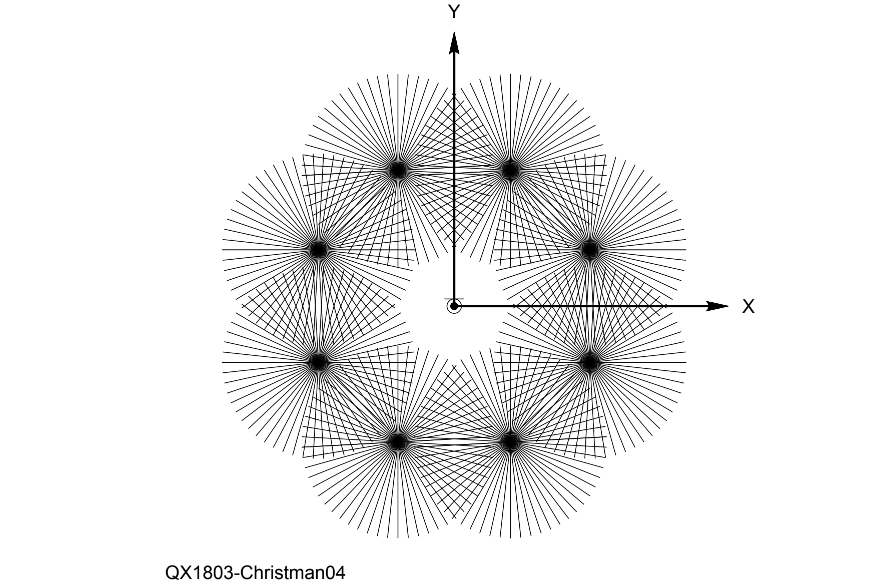

Figure 4 — Plan view of an 8-circle array which utilizes "High Accuracy" ground. Each element includes a ground-screen composed of 60 buried radials that are 57 feet long. The monopoles are constructed from #10 AWG copper wire, and the radials are #14 AWG copper. The radius of the circle is 81 feet, same as the model shown in Figure 1.

of gain at an elevation angle of 23.2° with a FBR of 18.1 dB. We can see that the elevation-plane FBR of the 8-circle array is only slightly better than that of the 4-square, but it provides a significant 2.44 dB of additional gain.

Detailed Computer Models

Next, I created another model of the "MiniNEC-style" 8-circle array described above, but this time I used the "High Accuracy" ground for the EZNEC analysis, which allowed me to include buried radials in the simulation. Figure 4 is a plan view of the antenna, showing the positioning of the eight elements with their associated ground-screens. The numbering of the various monopoles in this drawing is the same as in Figure 1.

Each element is made from #10 AWG copper wire, and has a ground-screen composed of sixty #14 AWG copper radials that are 57 feet long. In order to avoid "clashing" — where the radials from one vertical monopole intersect those of an adjacent element — the radials on the odd-numbered monopoles are buried 2 inches deep, while those on the even-numbered elements are 4 inches deep. Even with this strategy, the length of the radials had to be kept shorter than 0.25 λ to prevent those of monopole #1 from "clashing" with those from elements #3 and #7. The same holds true for the even-numbered monopoles.

The overall height of each element was "pruned" to achieve resonance at f = 3790 kHz. Since their radials were buried at slightly-different depths, the resonant height of the odd-numbered monopoles (63.11 feet) was not the same as that of the even-numbered elements (63.03 feet). With the circle radius fixed at 81 feet, I found that I had to tweak the phase-angle of the currents fed into the bases of the front monopoles in order to maximize the performance of the "High Accuracy" version of the array. The angle of the current phase-lag had to be increased somewhat, from 110° to 113°, and the resulting principal-plane radiation patterns are shown in Figures 5 and 6. This array has a peak forward gain of 8.42 dBi at 24.1° take-off angle, and the FBR is 18.1 dB. Table 25 compares the performance of this design with what was derived earlier from the antenna that utilizes "MiniNEC-style" ground. The two outcomes are very similar in many ways. Since a real-world 8-circle array installation would probably include a radial ground-screen, I will employ the "High-Accuracy" version of the antenna throughout the remainder of this article.

Omni-directional Configuration

If good coverage in all compass directions is desired, then the best solution is to feed just one of the eight monopoles in the array, while simultaneously "floating" the bases of the remaining seven elements. Figures 7 and 8 show the radiation patterns when monopole #1 is driven, with the elevation-plane pattern taken along a North-South azimuth. Notice that there is a slight amount of non-circularity in the azimuthal plane, amounting to roughly 0.8 dB.

If we decide to apply in-phase excitation to all eight elements, then the resulting azimuthal pattern is circular, but peak gain now occurs at a take-off angle of almost 49°! Feeding just one monopole yields more gain at low elevation angles. Finally, if we choose to drive the four odd-numbered (or even-numbered) elements, the azimuthal pattern resembles a square instead of a circle, and peak elevation-plane radiation once again takes place at about 49° take-off angle.

CW Operation

This array also performs well in the DX CW sub-band, if we simply alter the phase-angle of the current drive to the two front elements. Increasing the phase-lag angle from 113° to 118° produces good results, as illustrated by the radiation patterns displayed in Figures 9 and 10. At a frequency of 3510 kHz, the peak forward gain has fallen slightly, to 8.14 dBi at 23.9° take-off angle, while the front-to-back ratio has risen a bit to 18.5 dB. Table 26 lists the performance parameters of the 8-circle array on both the CW and SSB DX sub-bands. If omni-directional coverage is desired on CW, feeding monopole #1 by itself works well, as was true on phone. The amount of non-circularity in the azimuthal-plane radiation pattern is roughly 0.6 dB. Overall, the patterns look very similar to those shown for the SSB mode in Figures 7 and 8, so they will not be given here.

Designing for Other Frequencies

The basic 8-circle design can easily be re-scaled to work at a different frequency. The formula to use is:

$$\text{New radius} = (\text{Old radius})\frac{\text{Old Frequency}}{\text{New frequency}}$$

For example, if we wish to re-scale an array with an 81-foot radius, operating at 3790 kHz, to a frequency of 1830 kHz on Top Band, then:

$$\text{New radius} = (\text{Old radius})\frac{\text{Old Frequency}}{\text{New frequency}}$$

$$= (81 \text{ ft})\frac{3790}{1830} = 167.75 \text{ ft.}$$

Conclusions

This article has examined the performance of the "8-circle" phased-vertical array, in order to determine the impact of varying the radius of the circle, as well as the phase-angle of the feed-point current delivered to the two front elements. Important parameters (such as forward gain, take-off angle, front-to-back ratio, and input resistance) have been discussed, along with a method for achieving omni-directional radiation. Computer analysis indicates that an array which is designed for operation on 75-meter SSB may also be utilized successfully on 80-meter CW, although the gain is slightly reduced.

Al Christman was first licensed in 1974 as WA3WZD. He received his Doctorate in Electrical and Computer Engineering from Ohio University and is Professor of Electrical Engineering at Grove City College in Western Pennsylvania. When not modeling antennas by computer for fun, Al chases SSB DX on 20 and 80 meters, or enjoys ragchewing and contesting.

Notes

[1]EZNEC antenna-simulation software is available from Roy Lewallen, W7EL, P. O. Box 6658, Beaverton, OR 97007.

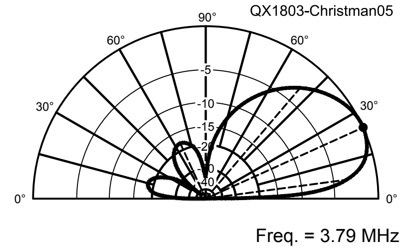

Figure 5 — Elevation-plane radiation pattern for the "best" 8-circle array design, using "High Accuracy" ground. Circle radius is 81 feet, $I_{front} = 1\ \angle{-113°}$ and $I_{back} = 1\ \angle 0°$. Frequency is 3790 kHz, peak forward gain = 8.42 dBi at 24.1° take-off angle, front-to-back ratio = 18.1 dB, $Z_{in(front)} = 39.3 + j8.51\ \Omega$ and $Z_{in(back)} = 7.32 - j5.74\ \Omega$.

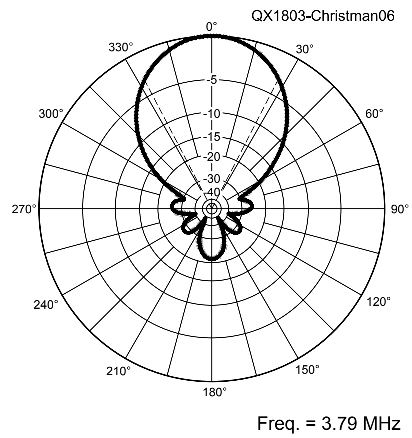

Figure 6 — Azimuth-plane radiation pattern for the "best" 8-circle array design, using "High Accuracy" ground. Circle radius is 81 feet, $I_{front} = 1\ \angle{-113°}$ and $I_{back} = 1\ \angle 0°$. Frequency is 3790 kHz, front to back ratio is 20.8 dB, at 24.1° take-off angle, front to side ratio is 25.2 dB at 24.1° take-off angle, half-power beamwidth is 54.6° at 24.1° take-off angle.

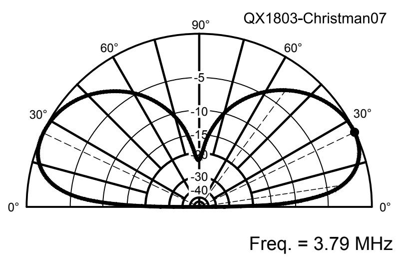

Figure 7 — Elevation-plane radiation pattern for the "best" 8-circle array design, using "High Accuracy" ground, when configured for omni-directional coverage in the azimuth plane. $I_1 = 1\ \angle 0°$ and I_2 through $I_8 = 0$. Frequency is 3790 kHz, peak gain is 0.80 dBi at 25.3° take-off angle, front-to-back ratio is 0 dB in the North-South direction, $Z_{in(1)} = 37.3 + j0.26\ \Omega$.

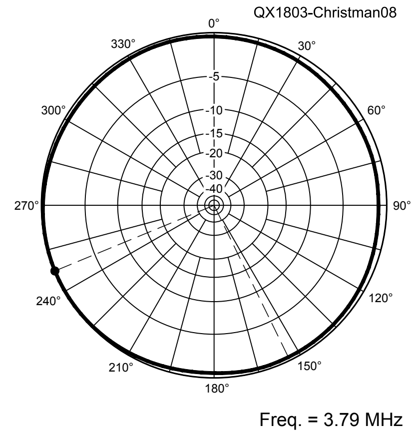

Figure 8 — Azimuth-plane radiation pattern for the "best" 8-circle array design, using "High Accuracy" ground, when configured for omni-directional coverage. $I_1 = 1\ \angle 0°$ and I_2 through $I_8 = 0$. Frequency is 3790 kHz, non-circularity is 0.79 dBi at 25.3° take-off angle.

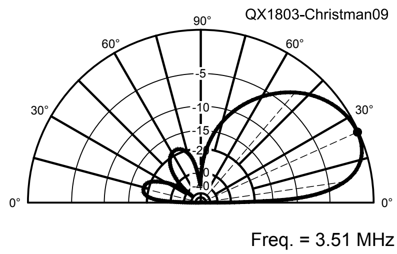

Figure 9 — Elevation-plane radiation pattern for the "best" 8-circle array design, using "High Accuracy" ground. Circle radius is 81 feet, $I_{front} = 1\ \angle{-118°}$ and $I_{back} = 1\ \angle 0°$, frequency is 3510 kHz, peak forward gain = 8.14 dBi at 23.9° take-off angle, front-to-back ratio is 18.5 dB, $Z_{in(front)} = 32.9 - j52.3\ \Omega$ and $Z_{in(back)} = 4.33 - j66.9\ \Omega$.

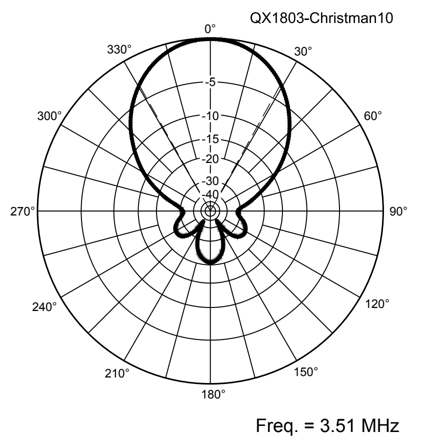

Figure 10 — Azimuth-plane radiation pattern for the "best" 8-circle array design, using "High Accuracy" ground. Circle radius is 81 feet, $I_{front} = 1\angle{-118°}$ and $I_{back} = 1\ \angle 0°$, frequency is 3510 kHz, front-to-back ratio is 20.6 dB at 23.9° take-off angle, front-to-side ratio is 24.8 dB at 23.9° take-off angle, half-power beamwidth is 58.4° at 23.9° take-off angle.

Table 1.

Performance of an 8-circle array whose radius is 70 feet, when operating at a frequency of 3790 kHz. The antenna is constructed from 8"-diameter aluminum conductors and placed over MiniNEC-style ground, with a conductivity of 0.005 S/m and dielectric constant of 13. Under the "Azimuthal Plane" heading, *either* the front-to-back ratio, designated with a (B) or the front-to-side ratio, designated with an (S) is shown, whichever is smaller (worse).

Columns 2 – 4, Elevation plane; columns 5 – 6, Azimuthal plane.

I_f, deg	*G_m, dBi*	*TOA, deg*	*FBR, dB*	*FBR or FSR, dB*	*HPBW, deg*	*$R_{in(back)}$, Ω*
–90	7.58	23.6	12.9	15.9 (S)	62.0	6.35
–95	7.68	23.5	13.9	17.8 (S)	61.6	5.47
–100	7.77	23.4	15.0	19.7 (S)	61.4	4.74
–105	7.84	23.3	16.1	21.8 (S)	61.0	4.17
–110	7.90	23.2	17.3	24.1 (S)	60.8	3.77
–115	7.94	23.0	18.5	21.9 (B)	60.4	3.54
–120	7.96	22.9	16.8	17.8 (B)	60.0	3.48
–125	7.97	22.8	14.3	15.0 (B)	59.6	3.59

Table 2.

Performance of an 8-circle array whose radius is 71 feet, when operating at a frequency of 3790 kHz. The antenna is constructed from 8"-diameter aluminum conductors and placed over MiniNEC-style ground, with a conductivity of 0.005 S/m and dielectric constant of 13. Under the "Azimuthal Plane" heading, *either* the front-to-back ratio, designated with a (B) or the front-to-side ratio, designated with an (S) is shown, whichever is smaller (worse).

Columns 2 – 4, Elevation plane; columns 5 – 6, Azimuthal plane.

I_f, deg	*G_m, dBi*	*TOA, deg*	*FBR, dB*	*FBR or FSR, dB*	*HPBW, deg*	*$R_{in(back)}$, Ω*
–90	7.66	23.6	13.0	16.2 (S)	61.2	6.41
–95	7.75	23.6	14.0	18.0 (S)	61.0	5.56
–100	7.84	23.4	15.1	20.1 (S)	60.6	4.86
–105	7.91	23.3	16.2	22.2 (S)	60.2	4.32
–110	7.96	23.1	17.4	24.6 (S)	60.0	3.95
–115	8.00	23.0	18.6	21.3 (B)	59.6	3.74
–120	8.02	22.9	16.5	17.4 (B)	59.2	3.69
–125	8.02	22.8	14.1	14.7 (B)	59.0	3.81

Table 3.

Performance of an 8-circle array whose radius is 72 feet, when operating at a frequency of 3790 kHz. The antenna is constructed from 8"-diameter aluminum conductors and placed over MiniNEC-style ground, with a conductivity of 0.005 S/m and dielectric constant of 13. Under the "Azimuthal Plane" heading, *either* the front-to-back ratio, designated with a (B) or the front-to-side ratio, designated with an (S) is shown, whichever is smaller (worse).

Columns 2 – 4, Elevation plane; columns 5 – 6, Azimuthal plane.

I_f, deg	*G_m, dBi*	*TOA, deg*	*FBR, dB*	*FBR or FSR, dB*	*HPBW, deg*	*$R_{in(back)}$, Ω*
–90	7.73	23.7	13.1	16.4 (S)	60.4	6.48
–95	7.82	23.5	14.2	18.4 (S)	60.0	5.66
–100	7.90	23.4	15.2	20.4 (S)	59.8	4.99
–105	7.97	23.3	16.4	22.6 (S)	59.4	4.48
–110	8.02	23.2	17.5	25.0 (S)	59.2	4.13
–115	8.06	23.0	18.8	20.7 (B)	58.8	3.94
–120	8.08	22.9	16.1	17.1 (B)	58.4	3.91
–125	8.07	22.8	13.8	14.4 (B)	58.2	4.04

Table 4.

Performance of an 8-circle array whose radius is 73 feet, when operating at a frequency of 3790 kHz. The antenna is constructed from 8"-diameter aluminum conductors and placed over MiniNEC-style ground, with a conductivity of 0.005 S/m and dielectric constant of 13. Under the "Azimuthal Plane" heading, *either* the front-to-back ratio, designated with a (B) or the front-to-side ratio, designated with an (S) is shown, whichever is smaller (worse).

Columns 2 – 4, Elevation plane; columns 5 – 6, Azimuthal plane.

I_f, deg	*G_m, dBi*	*TOA, deg*	*FBR, dB*	*FBR or FSR, dB*	*HPBW, deg*	*$R_{in(back)}$, Ω*
–90	7.79	23.7	13.2	16.7 (S)	59.6	6.56
–95	7.89	23.6	14.3	18.6 (S)	59.4	5.77
–100	7.97	23.4	15.4	20.7 (S)	59.0	5.13
–105	8.03	23.3	16.5	23.0 (S)	58.8	4.65
–110	8.08	23.2	17.6	25.3 (B)	58.4	4.32
–115	8.11	23.1	18.6	20.2 (B)	58.2	4.14
–120	8.13	23.0	15.8	16.7 (B)	57.8	4.13
–125	8.12	22.8	13.6	14.1 (B)	57.4	4.28

Table 5.

Performance of an 8-circle array whose radius is 74 feet, when operating at a frequency of 3790 kHz. The antenna is constructed from 8”-diameter aluminum conductors and placed over MiniNEC-style ground, with a conductivity of 0.005 S/m and dielectric constant of 13. Under the “Azimuthal Plane” heading, *either* the front-to-back ratio, designated with a (B) or the front-to-side ratio, designated with an (S) is shown, whichever is smaller (worse).

Columns 2 – 4, Elevation plane; columns 5 – 6, Azimuthal plane.

I_f, deg	G_m, dBi	TOA, deg	FBR, dB	FBR or FSR, dB	HPBW, deg	$R_{in(back)}$, Ω
–90	7.86	23.7	13.3	17.0 (S)	58.8	6.66
–95	7.95	23.6	14.4	18.9 (S)	58.6	5.90
–100	8.03	23.5	15.5	21.0 (S)	58.2	5.29
–105	8.09	23.3	16.6	23.3 (S)	58.0	4.82
–110	8.14	23.2	17.8	24.5 (B)	57.6	4.51
–115	8.17	23.1	18.2	19.6 (B)	57.4	4.36
–120	8.18	23.0	15.5	16.4 (B)	57.2	4.36
–125	8.17	22.8	13.4	13.9 (B)	56.8	4.52

Table 6.

Performance of an 8-circle array whose radius is 75 feet, when operating at a frequency of 3790 kHz. The antenna is constructed from 8”-diameter aluminum conductors and placed over MiniNEC-style ground, with a conductivity of 0.005 S/m and dielectric constant of 13. Under the “Azimuthal Plane” heading, *either* the front-to-back ratio, designated with a (B) or the front-to-side ratio, designated with an (S) is shown, whichever is smaller (worse).

Columns 2 – 4, Elevation plane; columns 5 – 6, Azimuthal plane.

I_f, deg	G_m, dBi	TOA, deg	FBR, dB	FBR or FSR, dB	HPBW, deg	$R_{in(back)}$, Ω
–90	7.92	23.7	13.4	17.2 (S)	58.2	6.77
–95	8.01	23.6	14.5	19.2 (S)	57.8	6.04
–100	8.08	23.5	15.6	21.4 (S)	57.6	5.45
–105	8.15	23.3	16.7	23.7 (S)	57.2	5.01
–110	8.19	23.2	17.9	23.7 (B)	57.0	4.72
–115	8.22	23.1	17.8	19.2 (B)	56.8	4.58
–120	8.23	23.0	15.2	16.0 (B)	56.4	4.59
–125	8.22	22.8	13.1	13.6 (B)	56.0	4.76

Table 7.

Performance of an 8-circle array whose radius is 76 feet, when operating at a frequency of 3790 kHz. The antenna is constructed from 8”-diameter aluminum conductors and placed over MiniNEC-style ground, with a conductivity of 0.005 S/m and dielectric constant of 13. Under the “Azimuthal Plane” heading, *either* the front-to-back ratio, designated with a (B) or the front-to-side ratio, designated with an (S) is shown, whichever is smaller (worse).

Columns 2 – 4, Elevation plane; columns 5 – 6, Azimuthal plane.

I_f, deg	G_m, dBi	TOA, deg	FBR, dB	FBR or FSR, dB	HPBW, deg	$R_{in(back)}$, Ω
–90	7.98	23.7	13.5	17.5 (S)	57.4	6.89
–95	8.07	23.6	14.6	19.5 (S)	57.2	6.19
–100	8.14	23.5	15.6	21.7 (S)	56.9	5.62
–105	8.20	23.3	16.8	24.0 (S)	56.6	5.20
–110	8.24	23.2	18.0	23.0 (B)	56.4	4.92
–115	8.27	23.1	17.4	18.7 (B)	56.0	4.80
–120	8.27	23.0	14.9	15.7 (B)	55.8	4.82
–125	8.26	22.9	12.9	13.4 (B)	55.4	5.00

Table 8.

Performance of an 8-circle array whose radius is 77 feet, when operating at a frequency of 3790 kHz. The antenna is constructed from 8”-diameter aluminum conductors and placed over MiniNEC-style ground, with a conductivity of 0.005 S/m and dielectric constant of 13. Under the “Azimuthal Plane” heading, *either* the front-to-back ratio, designated with a (B) or the front-to-side ratio, designated with an (S) is shown, whichever is smaller (worse).

Columns 2 – 4, Elevation plane; columns 5 – 6, Azimuthal plane.

I_f, deg	G_m, dBi	TOA, deg	FBR, dB	FBR or FSR, dB	HPBW, deg	$R_{in(back)}$, Ω
–90	8.03	23.8	13.6	17.8 (S)	56.8	7.03
–95	8.12	23.6	14.7	19.8 (S)	56.4	6.35
–100	8.19	23.5	15.8	22.0 (S)	56.2	5.80
–105	8.25	23.4	16.9	24.3 (S)	56.0	5.40
–110	8.29	23.2	18.1	22.3 (B)	55.6	5.14
–115	8.31	23.1	17.0	18.3 (B)	55.4	5.03
–120	8.32	23.0	14.7	15.4 (B)	55.0	5.06
–125	8.30	22.9	12.7	13.2 (B)	54.8	5.24

Table 9.

Performance of an 8-circle array whose radius is 78 feet, when operating at a frequency of 3790 kHz. The antenna is constructed from 8"-diameter aluminum conductors and placed over MiniNEC-style ground, with a conductivity of 0.005 S/m and dielectric constant of 13. Under the "Azimuthal Plane" heading, *either* the front-to-back ratio, designated with a (B) or the front-to-side ratio, designated with an (S) is shown, whichever is smaller (worse).

Columns 2 – 4, Elevation plane; columns 5 – 6, Azimuthal plane.

I_f, deg	*G_m, dBi*	*TOA, deg*	*FBR, dB*	*FBR or FSR, dB*	*HPBW, deg*	*$R_{in(back)}$, Ω*
–90	8.09	23.8	13.7	18.0 (S)	56.0	7.18
–95	8.17	23.7	14.8	20.1 (S)	55.8	6.52
–100	8.24	23.5	15.8	22.3 (S)	55.6	5.99
–105	8.30	23.4	17.0	23.6 (S)	55.2	5.61
–110	8.34	23.3	18.2	21.8 (B)	55.0	5.36
–115	8.36	23.1	16.8	17.9 (B)	54.8	5.26
–120	8.36	23.0	14.4	15.1 (B)	54.4	5.30
–125	8.34	22.8	12.5	13.0 (B)	54.2	5.49

Table 10.

Performance of an 8-circle array whose radius is 79 feet, when operating at a frequency of 3790 kHz. The antenna is constructed from 8"-diameter aluminum conductors and placed over MiniNEC-style ground, with a conductivity of 0.005 S/m and dielectric constant of 13. Under the "Azimuthal Plane" heading, *either* the front-to-back ratio, designated with a (B) or the front-to-side ratio, designated with an (S) is shown, whichever is smaller (worse).

Columns 2 – 4, Elevation plane; columns 5 – 6, Azimuthal plane.

I_f, deg	*G_m, dBi*	*TOA, deg*	*FBR, dB*	*FBR or FSR, dB*	*HPBW, deg*	*$R_{in(back)}$, Ω*
–90	8.13	23.8	13.8	18.3 (S)	55.6	7.34
–95	8.22	23.7	14.8	20.4 (S)	55.2	6.70
–100	8.29	23.5	15.9	21.9 (S)	54.8	6.19
–105	8.34	23.4	17.1	22.2 (S)	54.6	5.82
–110	8.38	23.3	18.2	21.2 (B)	54.4	5.59
–115	8.40	23.1	16.4	17.5 (B)	54.0	5.50
–120	8.40	23.0	14.2	14.9 (B)	53.8	5.55
–125	8.38	22.9	12.3	12.8 (B)	53.6	5.74

Table 11.

Performance of an 8-circle array whose radius is 80 feet, when operating at a frequency of 3790 kHz. The antenna is constructed from 8"-diameter aluminum conductors and placed over MiniNEC-style ground, with a conductivity of 0.005 S/m and dielectric constant of 13. Under the "Azimuthal Plane" heading, *either* the front-to-back ratio, designated with a (B) or the front-to-side ratio, designated with an (S) is shown, whichever is smaller (worse).

Columns 2 – 4, Elevation plane; columns 5 – 6, Azimuthal plane.

I_f, deg	*G_m, dBi*	*TOA, deg*	*FBR, dB*	*FBR or FSR, dB*	*HPBW, deg*	*$R_{in(back)}$, Ω*
–90	8.18	23.8	13.9	18.6 (S)	54.8	7.51
–95	8.26	23.7	14.9	20.4 (S)	54.6	6.89
–100	8.33	23.6	16.0	20.7 (S)	54.4	6.40
–105	8.38	23.4	17.1	20.9 (S)	54.0	6.05
–110	8.42	23.3	18.3	20.6 (B)	53.8	5.83
–115	8.44	23.2	16.1	17.2 (B)	53.4	5.74
–120	8.44	23.0	13.9	14.6 (B)	53.2	5.80
–125	8.42	22.9	12.1	12.6 (B)	53.0	5.99

Table 12.

Performance of an 8-circle array whose radius is 81 feet, when operating at a frequency of 3790 kHz. The antenna is constructed from 8"-diameter aluminum conductors and placed over MiniNEC-style ground, with a conductivity of 0.005 S/m and dielectric constant of 13. Under the "Azimuthal Plane" heading, *either* the front-to-back ratio, designated with a (B) or the front-to-side ratio, designated with an (S) is shown, whichever is smaller (worse).

Columns 2 – 4, Elevation plane; columns 5 – 6, Azimuthal plane.

I_f, deg	*G_m, dBi*	*TOA, deg*	*FBR, dB*	*FBR or FSR, dB*	*HPBW, deg*	*$R_{in(back)}$, Ω*
–90	8.22	23.9	14.0	18.8 (S)	54.2	7.69
–95	8.30	23.7	15.0	19.3 (S)	54.0	7.09
–100	8.37	23.6	16.1	19.6 (S)	53.6	6.62
–105	8.42	23.4	17.2	19.8 (S)	53.4	6.28
–110	8.46	23.3	18.4	20.1 (B)	53.2	6.07
–115	8.48	23.2	15.8	16.8 (B)	52.8	5.99
–120	8.48	23.0	13.7	14.3 (B)	52.6	6.05
–125	8.45	22.9	11.9	12.3 (B)	52.4	6.25

Table 13.

Performance of an 8-circle array whose radius is 82 feet, when operating at a frequency of 3790 kHz. The antenna is constructed from 8”-diameter aluminum conductors and placed over MiniNEC-style ground, with a conductivity of 0.005 S/m and dielectric constant of 13. Under the “Azimuthal Plane” heading, *either* the front-to-back ratio, designated with a (B) or the front-to-side ratio, designated with an (S) is shown, whichever is smaller (worse).

Columns 2 – 4, Elevation plane; columns 5 – 6, Azimuthal plane.

I_f, deg	G_m, dBi	TOA, deg	FBR, dB	FBR or FSR, dB	HPBW, deg	$R_{in(back)}$, Ω
−90	8.26	23.9	14.1	18.1 (S)	53.6	7.88
−95	8.34	23.7	15.1	18.3 (S)	53.4	7.30
−100	8.41	23.6	16.2	18.6 (S)	53.0	6.84
−105	8.46	23.5	17.3	18.9 (S)	52.8	6.51
−110	8.49	23.3	18.1	19.2 (S)	52.6	6.31
−115	8.51	23.2	15.5	16.5 (B)	52.2	6.24
−120	8.51	23.0	13.4	14.1 (B)	52.0	6.31
−125	8.49	22.9	11.7	12.2 (B)	51.6	6.51

Table 14.

Performance of an 8-circle array whose radius is 83 feet, when operating at a frequency of 3790 kHz. The antenna is constructed from 8”-diameter aluminum conductors and placed over MiniNEC-style ground, with a conductivity of 0.005 S/m and dielectric constant of 13. Under the “Azimuthal Plane” heading, *either* the front-to-back ratio, designated with a (B) or the front-to-side ratio, designated with an (S) is shown, whichever is smaller (worse).

Columns 2 – 4, Elevation plane; columns 5 – 6, Azimuthal plane.

I_f, deg	G_m, dBi	TOA, deg	FBR, dB	FBR or FSR, dB	HPBW, deg	$R_{in(back)}$, Ω
−90	8.29	23.9	14.1	17.2 (S)	53.0	8.08
−95	8.37	23.8	15.2	17.5 (S)	52.8	7.52
−100	8.44	23.6	16.3	17.7 (S)	52.4	7.07
−105	8.49	23.5	17.4	18.0 (S)	52.2	6.75
−110	8.53	23.3	17.7	18.3 (S)	52.0	6.56
−115	8.54	23.2	15.2	16.2 (B)	51.8	6.50
−120	8.54	23.1	13.2	13.8 (B)	51.4	6.57
−125	8.52	22.9	11.5	12.0 (B)	51.2	6.77

Table 15.

Performance of an 8-circle array whose radius is 84 feet, when operating at a frequency of 3790 kHz. The antenna is constructed from 8”-diameter aluminum conductors and placed over MiniNEC-style ground, with a conductivity of 0.005 S/m and dielectric constant of 13. Under the “Azimuthal Plane” heading, *either* the front-to-back ratio, designated with a (B) or the front-to-side ratio, designated with an (S) is shown, whichever is smaller (worse).

Columns 2 – 4, Elevation plane; columns 5 – 6, Azimuthal plane.

I_f, deg	G_m, dBi	TOA, deg	FBR, dB	FBR or FSR, dB	HPBW, deg	$R_{in(back)}$, Ω
−90	8.32	23.9	14.2	16.4 (S)	52.4	8.30
−95	8.40	23.8	15.3	16.6 (S)	52.2	7.74
−100	8.47	23.6	16.4	16.9 (S)	52.0	7.31
−105	8.52	23.5	17.5	17.2 (S)	51.6	7.00
−110	8.55	23.4	17.3	17.5 (S)	51.4	6.82
−115	8.57	23.2	15.0	15.8 (B)	51.2	6.76
−120	8.57	23.1	13.0	13.6 (B)	50.8	6.83
−125	8.54	23.0	11.4	11.8 (B)	50.6	7.03

Table 16.

Performance of an 8-circle array whose radius is 85 feet, when operating at a frequency of 3790 kHz. The antenna is constructed from 8”-diameter aluminum conductors and placed over MiniNEC-style ground, with a conductivity of 0.005 S/m and dielectric constant of 13. Under the “Azimuthal Plane” heading, *either* the front-to-back ratio, designated with a (B) or the front-to-side ratio, designated with an (S) is shown, whichever is smaller (worse).

Columns 2 – 4, Elevation plane; columns 5 – 6, Azimuthal plane.

I_f, deg	G_m, dBi	TOA, deg	FBR, dB	FBR or FSR, dB	HPBW, deg	$R_{in(back)}$, Ω
−90	8.35	23.9	14.3	15.6 (S)	51.8	8.52
−95	8.43	23.8	15.3	15.9 (S)	51.6	7.98
−100	8.50	23.6	16.4	16.2 (S)	51.4	7.56
−105	8.55	23.5	17.6	16.4 (S)	51.0	7.26
−110	8.58	23.4	17.0	16.8 (S)	50.8	7.08
−115	8.60	23.2	14.7	15.6 (B)	50.6	7.03
−120	8.59	23.1	12.8	13.4 (B)	50.4	7.10
−125	8.57	23.0	11.2	11.6 (B)	50.0	7.30

DX ENGINEERING

Showroom Staffing Hours:
9 am to 5 pm ET, Monday-Saturday

Ordering (via phone):
8:30 am to midnight ET, Monday-Friday
8:30 am to 5 pm ET, Weekends

Phone or e-mail Tech Support: 330-572-3200
8:30 am to 7 pm ET, Monday-Friday
9:00 am to 5 pm ET, Saturday
All Times Eastern I Country Code: +1
DXEngineering@DXEngineering.com

800-777-0703 | DXEngineering.com

Get the Best Antennas Fast and for Less at DX Engineering!

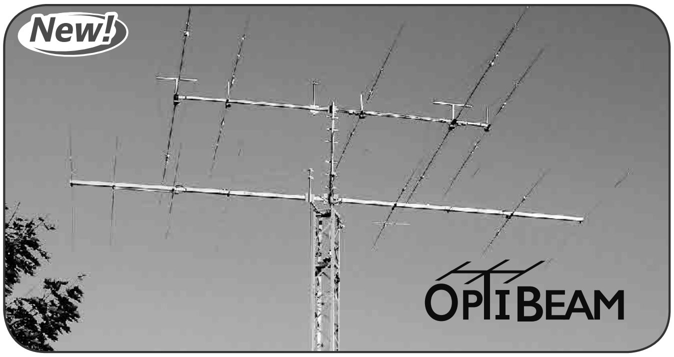

OptiBeam Antennas

DX Engineering is now the exclusive North American retailer of HF directional antennas from OptiBeam. Proven in stations around the globe, OptiBeam's German-engineered, handcrafted directional mono-band and multiband Yagi and log cell Yagi antennas deliver the highest possible gain, cleanest radiation patterns, optimum band coverage, and power handling without compromise. DX Engineering offers all OptiBeam Amateur Radio antennas. Popular models are in stock and ready for fast shipment. Order today!

Ciro Mazzoni Radiocomunicazioni

Ciro Mazzoni Baby and Midi Loop Antennas

Founded in Verona, Italy, Ciro Mazzoni Radiocomunicazioni has been a trusted supplier of professional-quality radio communications equipment for more than 40 years. DX Engineering is pleased to offer Ciro Mazzoni's popular magnetic Baby Loop and Midi Loop antennas. Compact, quiet and easy to install, the sturdy Baby Loop (6.6-29.8 MHz) and Midi Loop (3.5-14.5 MHz) are designed and manufactured to meet the highest standards for performance and reliability. Look for them at DXEngineering.com.

MZZ-BABY $2,097.99 *MZZ-MIDI $2,479.99*

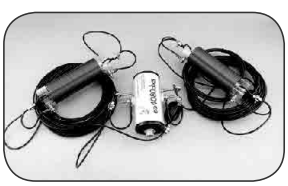

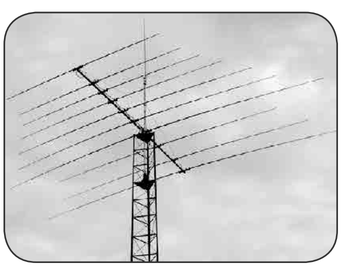

EA ANTENNA

EAntenna

Exclusively offered in North America by DX Engineering, EAntenna boasts an exciting lineup of rugged HF and VHF antennas, including Yagi, log periodic, rotatable dipole and vertical models. These antennas combine cutting-edge computer modeling optimization with robust mechanical and electrical designs to deliver high performance at a budget-friendly price. Choose from mono-band and multiband beams, low-noise loop fed arrays, optimized wideband arrays, and many more used by some of the world's most competitive contesters.

DX ENGINEERING

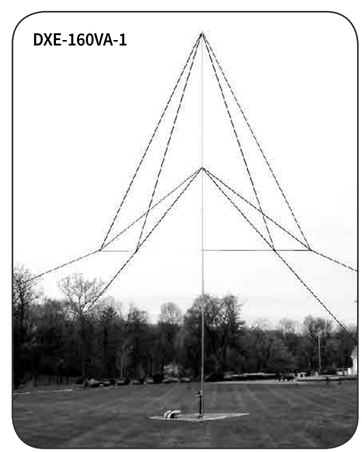

DX Engineering Antennas

When you demand durability, superior construction and proven performance, DX Engineering antennas rank high on all fronts. Select from the Skyhawk™ Tri-Band Yagi and Skylark Dual-Band Yagi; the Active Magnetic Loop MF/HF receiving antenna; 75/80 meter monoband verticals; 160 meter monoband vertical; 2-, 6- and 9-band vertical Butternut HF verticals now made by DX Engineering; the THUNDERBOLT® 80/40 meter high-performance vertical; low-SWR, wide-bandwidth HEXX beams, and others. Plus, get every accessory you'll ever need at one convenient place.

YAESU ICOM KENWOOD ALINCO

Free Standard Shipping for Orders Over $99*. If your order, before tax, is over 99 bucks, then you won't spend a dime on shipping. (Additional special handling fees may be incurred for Hazardous Materials, Truck Freight, International Orders, Next Day Air, Oversize Shipments, etc.).

FAST FREE SHIPPING over $99*

Email Support 24/7/365 at DXEngineering@DXEngineering.com ***Stay connected:*** YouTube

Table 17.

Performance of an 8-circle array whose radius is 86 feet, when operating at a frequency of 3790 kHz. The antenna is constructed from 8"-diameter aluminum conductors and placed over MiniNEC-style ground, with a conductivity of 0.005 S/m and dielectric constant of 13. Under the "Azimuthal Plane" heading, *either* the front-to-back ratio, designated with a (B) or the front-to-side ratio, designated with an (S) is shown, whichever is smaller (worse).

Columns 2 – 4, Elevation plane; columns 5 – 6, Azimuthal plane.

I_f, deg	*G_m, dBi*	*TOA, deg*	*FBR, dB*	*FBR or FSR, dB*	*HPBW, deg*	*$R_{in(back)}$, Ω*
–90	8.37	24.0	14.4	15.0 (S)	51.4	8.75
–95	8.45	23.8	15.4	15.2 (S)	51.0	8.22
–100	8.52	23.7	16.5	15.5 (S)	50.8	7.81
–105	8.57	23.6	17.6	15.8 (S)	50.6	7.52
–110	8.60	23.4	16.6	16.1 (S)	50.4	7.35
–115	8.62	23.3	14.4	15.3 (B)	50.0	7.30
–120	8.62	23.1	12.6	13.2 (B)	49.8	7.37
–125	8.59	23.0	11.0	11.4 (B)	49.6	7.56

Table 18.

Performance of an 8-circle array whose radius is 87 feet, when operating at a frequency of 3790 kHz. The antenna is constructed from 8"-diameter aluminum conductors and placed over MiniNEC-style ground, with a conductivity of 0.005 S/m and dielectric constant of 13. Under the "Azimuthal Plane" heading, *either* the front-to-back ratio, designated with a (B) or the front-to-side ratio, designated with an (S) is shown, whichever is smaller (worse).

Columns 2 – 4, Elevation plane; columns 5 – 6, Azimuthal plane.

I_f, deg	*G_m, dBi*	*TOA, deg*	*FBR, dB*	*FBR or FSR, dB*	*HPBW, deg*	*$R_{in(back)}$, Ω*
–90	8.39	24.0	14.4	14.3 (S)	50.8	8.99
–95	8.47	23.8	15.5	14.6 (S)	50.6	8.47
–100	8.54	23.7	16.6	14.9 (S)	50.2	8.07
–105	8.59	23.6	17.7	15.2 (S)	50.0	7.78
–110	8.62	23.4	16.3	15.4 (S)	49.8	7.62
–115	8.64	23.3	14.2	15.0 (B)	49.6	7.57
–120	8.64	23.1	12.4	12.9 (B)	49.2	7.64
–125	8.61	23.0	10.8	11.2 (B)	49.0	7.83

Table 19.

Performance of an 8-circle array whose radius is 88 feet, when operating at a frequency of 3790 kHz. The antenna is constructed from 8"-diameter aluminum conductors and placed over MiniNEC-style ground, with a conductivity of 0.005 S/m and dielectric constant of 13. Under the "Azimuthal Plane" heading, *either* the front-to-back ratio, designated with a (B) or the front-to-side ratio, designated with an (S) is shown, whichever is smaller (worse).

Columns 2 – 4, Elevation plane; columns 5 – 6, Azimuthal plane.

I_f, deg	*G_m, dBi*	*TOA, deg*	*FBR, dB*	*FBR or FSR, dB*	*HPBW, deg*	*$R_{in(back)}$, Ω*
–90	8.41	24.0	14.5	13.7 (S)	50.2	9.24
–95	8.49	23.9	15.6	14.0 (S)	50.0	8.73
–100	8.56	23.7	16.6	14.3 (S)	49.8	8.34
–105	8.61	23.6	17.8	14.6 (S)	49.4	8.06
–110	8.64	23.5	16.0	14.9 (S)	49.2	7.89
–115	8.66	23.3	13.9	14.7 (B)	49.0	7.85
–120	8.65	23.2	12.2	12.7 (B)	48.8	7.92
–125	8.63	23.0	10.7	11.0 (B)	48.4	8.11

Table 20.

Performance of an 8-circle array whose radius is 89 feet, when operating at a frequency of 3790 kHz. The antenna is constructed from 8"-diameter aluminum conductors and placed over MiniNEC-style ground, with a conductivity of 0.005 S/m and dielectric constant of 13. Under the "Azimuthal Plane" heading, *either* the front-to-back ratio, designated with a (B) or the front-to-side ratio, designated with an (S) is shown, whichever is smaller (worse).

Columns 2 – 4, Elevation plane; columns 5 – 6, Azimuthal plane.

I_f, deg	*G_m, dBi*	*TOA, deg*	*FBR, dB*	*FBR or FSR, dB*	*HPBW, deg*	*$R_{in(back)}$, Ω*
–90	8.42	24.1	14.6	13.2 (S)	49.8	9.50
–95	8.50	23.9	15.6	13.4 (S)	49.6	9.00
–100	8.57	23.8	16.7	13.7 (S)	49.2	8.61
–105	8.62	23.6	17.8	14.0 (S)	49.0	8.34
–110	8.65	23.5	15.6	14.3 (S)	48.8	8.17
–115	8.67	23.3	13.6	14.4 (B)	48.4	8.13
–120	8.67	23.1	12.0	12.5 (B)	48.2	8.20
–125	8.64	23.0	10.5	10.9 (B)	48.0	8.38

Table 21.

Performance of an 8-circle array whose radius is 90 feet, when operating at a frequency of 3790 kHz. The antenna is constructed from 8"-diameter aluminum conductors and placed over MiniNEC-style ground, with a conductivity of 0.005 S/m and relative dielectric constant of 13. Under the "Azimuthal Plane" heading, *either* the front-to-back ratio, designated with a (B) or the front-to-side ratio, designated with an (S) is shown, whichever is smaller (worse).

Columns 2 – 4, Elevation plane; columns 5 – 6, Azimuthal plane.

I_f, deg	*G_m, dBi*	*TOA, deg*	*FBR, dB*	*FBR or FSR, dB*	*HPBW, deg*	*$R_{in(back)}$, Ω*
–90	8.43	24.1	14.6	12.7 (S)	49.2	9.76
–95	8.51	23.9	15.7	12.9 (S)	49.0	9.27
–100	8.58	23.8	16.8	13.2 (S)	48.8	8.89
–105	8.63	23.6	17.8	13.5 (S)	48.4	8.62
–110	8.66	23.5	15.3	13.8 (S)	48.2	8.46
–115	8.68	23.3	13.4	14.1 (S)	48.0	8.41
–120	8.68	23.2	11.8	12.3 (B)	47.8	8.48
–125	8.66	23.0	10.3	10.7 (B)	47.4	8.66

Table 22.

Performance of an 8-circle array driven using the classic quadrature-feed system, $I_{front} = 1 \angle\text{-}90°$ and $I_{back} = 1 \angle\text{-}0°$ when operating at a frequency of 3790 kHz. The antenna is constructed from 8 inch diameter aluminum conductors and placed over MiniNEC-style ground, with a conductivity of 0.005 S/m and a relative dielectric constant of 13.

Circle radius, ft	*G_m, elev., dBi*	*TOA, elev., deg*	*FBR, elev., dB*	*FSR, azim., dB*	*HPBW, azim., deg*	*$R_{in(back)}$, Ω*
70	7.58	23.6	12.9	15.9	62.0	6.35
71	7.66	23.6	13.0	16.2	61.2	6.41
72	7.73	23.7	13.1	16.4	60.4	6.48
73	7.79	23.7	13.2	16.7	59.6	6.56
74	7.86	23.7	13.3	17.0	58.8	6.66
75	7.92	23.7	13.4	17.2	58.2	6.77
76	7.98	23.7	13.5	17.5	57.4	6.89
77	8.03	23.8	13.6	17.8	56.8	7.03
78	8.09	23.8	13.7	18.0	56.0	7.18
79	8.13	23.8	13.8	18.3	55.6	7.34
80	8.18	23.8	13.9	18.6	54.8	7.51
81	8.22	23.9	14.0	18.8	54.2	7.69
82	8.26	23.9	14.1	18.1	53.6	7.88
83	8.29	23.9	14.1	17.2	53.0	8.08
84	8.32	23.9	14.2	16.4	52.4	8.30
85	8.35	23.9	14.3	15.6	51.8	8.52
86	8.37	24.0	14.4	15.0	51.4	8.75
87	8.39	24.0	14.4	14.3	50.8	8.99
88	8.41	24.0	14.5	13.7	50.2	9.24
89	8.42	24.1	14.6	13.2	49.8	9.50
90	8.43	24.1	14.6	12.7	49.2	9.76

Table 23.

Data for all of the 8-circle array configurations that can provide at least 18 dB of front-to-back ratio in the elevation plane, and at least 18 dB of FBR (or FSR) in the azimuthal plane. This list was compiled by reviewing all of the possible combinations that are shown in Tables 1 through 21.

Circle radius, ft	*Phase lag, deg*	*G_m, elev., dBi*	*TOA, elev., deg*	*FBR or FSR, elev, dB*	*FBR or FSR, azim dB*	*FBR or FSR, avg, dB*	*$R_{in(back)}$, Ω*
70	115	7.94	23.0	18.5	21.9	20.2	3.54
71	115	8.00	23.0	18.6	21.3	20.0	3.74
72	115	8.06	23.0	18.8	20.7	19.7	3.94
73	115	8.11	23.1	18.6	20.2	19.4	4.14
74	115	8.17	23.1	18.2	19.6	18.9	4.36
77	110	8.29	23.2	18.1	22.3	20.2	5.14
78	110	8.34	23.3	18.2	21.8	20.0	5.36
79	110	8.38	23.3	18.2	21.2	19.7	5.59
80	110	8.42	23.3	18.3	20.6	19.5	5.83
81	110	8.46	23.3	18.4	20.1	19.3	6.07
82	110	8.49	23.3	18.1	19.2	18.6	6.31

Table 24.

Data for 8-circle array configurations where the radius of the circle is held constant at 81 feet. Here the lag-angle for the input current fed to the bases of the front elements is varied slightly, compared to the original reference value of 110 degrees, which was found earlier (see Table 23).

Circle radius, ft	*Phase lag, deg*	*G_m, elev., dBi*	*TOA, elev., deg*	*FBR or FSR, elev., dB*	*FBR or FSR, azim., dB*	*FBR or FSR, avg., dB*	*$R_{in(back)}$, Ω*
81	109	8.45	23.3	18.2	20.1	19.1	6.10
81	110	8.46	23.3	18.4	20.1	19.3	6.07
81	111	8.46	23.3	17.9	19.4	18.6	6.04

Table 25.

A comparison of the computer-predicted performance of an 8-circle array of quarter-wave vertical elements, when the radius of the circle is 81 feet, at an operating frequency of 3790 kHz. One version of the EZNEC model utilizes "Mini-NEC-style" ground, and a phase-lag angle of 110 degrees for the input current to the front elements. The other model employs "High-Accuracy" ground with an extensive radial ground-screen, and a phase-lag angle of 113 degrees for the current into the front elements. In both cases, the soil has a conductivity of 0.005 S/m and a dielectric constant of 13.

Parameter	*Mini-NEC Ground*	*High-Accuracy Ground*
Peak gain and take-off angle	8.46 dBi at 23.3 deg	8.42 dBi at 24.1 deg
Elev. plane front-to-back ratio	18.4 dB	18.1 dB
Azim. plane front-to-back ratio	20.1 dB	20.8 dB
Azim. plane front-to-side ratio	20.2 dB	25.2 dB
Azim. plane half-power beamwidth	53.2 deg	54.6 deg
Input impedance front element	36.3 + j8.06 Ω	39.3 + j8.51 Ω
Input impedance back element	6.07 - j 6.19 Ω	7.32 - j5.74 Ω
Gain at 5 deg take-off angle	3.01 dBi	2.87 dBi
Gain at 10 deg take-off angle	6.51 dBi	6.38 dBi
Gain at 15 deg take-off angle	7.86 dBi	7.75 dBi
Gain at 20 deg take-off angle	8.38 dBi	8.30 dBi
Gain at 25 deg take-off angle	8.44 dBi	8.41 dBi
Gain at 30 deg take-off angle	8.19 dBi	8.22 dBi
Gain at 35 deg take-off angle	7.69 dBi	7.79 dBi
Gain at 40 deg take-off angle	6.97 dBi	7.16 dBi

Table 26.

A comparison of the computer-predicted performance of an 8-circle array on both the 80-meter CW and 75-meter SSB DX sub-bands, at frequencies of 3510 and 3790 kHz, respectively. The EZNEC "High-Accuracy" ground option is utilized in conjunction with an extensive radial ground-screen for each element. The underlying soil has a conductivity of 0.005 S/m and a dielectric constant of 13.

Parameter	*f = 3510 kHz*	*f = 3790 kHz*
Peak gain and take-off angle	8.14 dBi at 23.9 deg	8.42 dBi at 24.1 deg
Elev. plane front-to-back ratio	18.5 dB	18.1 dB
Azim. plane front-to-back ratio	20.6 dB	20.8 dB
Azim. plane front-to-side ratio	24.8 dB	25.2 dB
Azim. plane half-power beamwidth	58.4 deg	54.6 deg
Input impedance front element	32.9 - j52.3 Ω	39.3 + j8.51 Ω
Input impedance back element	4.33 - j66.9 Ω	7.32 - j5.74 Ω
Gain at 5 deg take-off angle	2.68 dBi	2.87 dBi
Gain at 10 deg take-off angle	6.15 dBi	6.38 dBi
Gain at 15 deg take-off angle	7.50 dBi	7.75 dBi
Gain at 20 deg take-off angle	8.04 dBi	8.30 dBi
Gain at 25 deg take-off angle	8.13 dBi	8.41 dBi
Gain at 30 deg take-off angle	7.93 dBi	8.22 dBi
Gain at 35 deg take-off angle	7.50 dBi	7.79 dBi
Gain at 40 deg take-off angle	6.86 dBi	7.16 dBi

Rudy Severns, N6LF

PO Box 589, Cottage Grove, OR 97424; **n6lf@arrl.net**

Insulated Wire and Antennas

N6LF studies the use of insulated versus bare copper wire, and concludes that leaving the insulation on the wire is generally benign, however, in certain cases with sparse radial systems there can be a substantial impact.

Insulated copper wire intended for home wiring is often used for antennas and ground systems. This wire is readily available at hardware and home improvement emporiums and often significantly less expensive than the equivalent wire without insulation. Among amateurs there has been a recurring discussion whether it's necessary or even useful to strip the insulation. Stripping a few hundred feet isn't a serious chore but if you're laying out a 160 m radial field with thousands of feet of wire then stripping would be a chore. Although this question has popped frequently for as long as ham radio has been around I've never seen careful discussion of the subject using both theory and experimental tests. Some years ago I wrote a pair of *QEX* articles[1, 2] discussing antenna wire but I didn't explore the dielectric loading effect of insulation, so I thought it might help to extend that discussion to include the effect of insulation. To answer some of the questions I used a combination of modeling and experimental results. I make no claim that this is a complete or final answer but it should at least provide food for thought.

Concerns

Our concerns fall into three categories:

1) Does the insulation introduce additional loss? Even if the loss for new wire is small, what happens to the loss after years of exposure to UV and weather?

2) Even if there is no loss, insulation will introduce some dielectric loading, i.e. the tuning of the antenna will be affected. Does this matter and can it introduce any serious problems?

3) Mechanical issues. What happens to the conductor as the insulation deteriorates, and oxidation, corrosion, follow? Because of it's larger diameter does an insulated wire build up a greater ice load in winter storms?

Plan of Attack

To evaluate insulation induced loss we can wind samples of wire into an air-core inductor and measure its Q. The Q of inductors with Q>100 are very sensitive to conductor loss. Even a small change in RF resistance is magnified as a change in Q. My Nov/Dec 2000 *QEX* article explained this in detail so I'll not repeat that information here but a PDF of the article can be found at: **www.antennasbyn6lf.com**. I used this approach again to test samples of new and old insulated wire.

To explore the effect of dielectric loading I used EZNEC Pro[3] with the NEC4.2 engine combined with Dan Maguire's AutoEZ EXCEL based program[4]. This raises the question "how much can we rely on NEC modeling?" That's a fundamental question, so last year I took a careful experimental look at this issue and reported my results in the Jul/Aug 2016 issue[5] of *QEX*, which makes a pretty good case for NEC, at least for low or buried wires with or without insulation. For the present discussion I'm going to assume the NEC modeling answers are good enough for us to make some judgments. The NEC *QEX* article is also available at **www.antennasbyn6lf.com**.

The Wire

This discussion will assume either solid #12 AWG or #14 AWG copper wire with THHN insulation because this is by far the most common and is representative of this class of wire. The insulation is PVC with a thin nylon coating. When exposed to UV and weather over extended periods the nylon coating usually flakes off and the color of the underlying PVC fades. Besides a roll of new wire, I had on hand thousands of feet of well exposed #12 AWG wire used for my 160 m vertical array and other antenna projects going back 20 years. In addition Guy Olinger, K2AV, sent me ten samples including insulated and bare, new and very weathered #14 AWG THHN. This allowed me to test both new and very weathered wires.

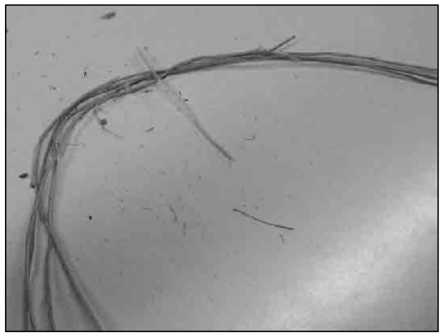

Figure 1 — Sample of degraded #12 AWG radial wire.

Test Inductor Results

Figure 1 shows a typical sample of used wire. Notice that the outer nylon cover is flaking off and the insulation is bleached (the original color was red). The insulation is brittle and the copper oxidized. I also happened to have the coil form used for the *QEX* wire article so I used that for the coil form using the same number of turns as before. This allowed me to compare the earlier work with the current. Each wire sample was wound on the coil form as shown in Figure 2. Q was measured with an HP4342A Q-meter as shown in Figure 3. An HP5334A frequency counter was used to determine the test frequency.

Tables 1 and 2 show the results. Samples R1 through R8 were weathered radials supplied by K2AV. The small variations in Q are to be expected with the informal winding.

I also measured the Q varying the frequency from 1.5 to 4.5 MHz on some new #14 AWG and sample R6 from K2AV as shown in Figure 4. Measurements for the two samples were almost identical so the graph is for R6. These experiments didn't appear to show any loss introduced by the insulation, either new or very weathered.

Insulated Dipoles

To see the dielectric loading effect of insulation we can use a dipole in free space and examine the feedpoint impedance as we change from bare to insulated wire. The relative dielectric constant ε_r is 3.2 for PVC and 4 for nylon. The nylon coating is very thin so it probably doesn't effect the totalt ε_r very much so I used ε_r of 3.3 as a compromise. The model was adjusted to be resonant at fr = 1.83 MHz using bare wire. Insulation was then added with the results shown in Table 3.

Adding insulation reduces fr from 1.830 MHz to 1.803 MHz due to dielectric loading. Since there are no losses in the model the shifts in Ri represent a change in radiation resistance Rr. Insulation changes both the feedpoint impedance and fr, reducing Ri from 72.2 to71.7 Ω as well as fr from 1.830 to 1.803 MHz. When the

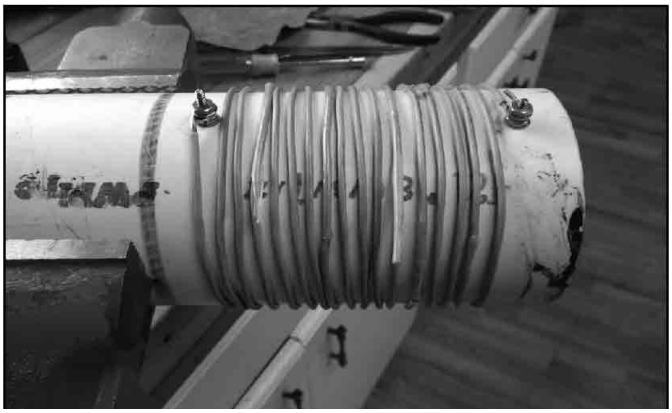

Figure 2 — Old radial wire wound into an inductor.

Figure 3 — HP4342A Q-meter shown on top of a vector impedance meter.

Table 1
Comparison of Q for N6LF #12 AWG wire.

wire	*Q at 1.8 MHz*	*Q at 3.9 MHz*
old #12 AWG	405	470
new #12 AWG	400	460

Table 2
Comparison of Q for K2AV #14 AWG wire at 3.6 MHz.

Wire	*Q*	*Wire*	*Q*
Bare	395	R4	400
New ins	390	R5	382
R1	394	R6	390
R2	396	R7	405
R3	398	R8	395

Table 3
160 m dipole in free space, ε_r=3.3.

wire, #12 AWG	*frequency, MHz*	*dipole length. ft*	*Ri, Ω*	*Xi, Ω*
bare	1.830	262.4	72.2	0
insulated	1.830	262.4	71.7	+27.9
insulated	1.803	262.4	70.3Ω	0
insulated	1.830	259.6	70.3Ω	0

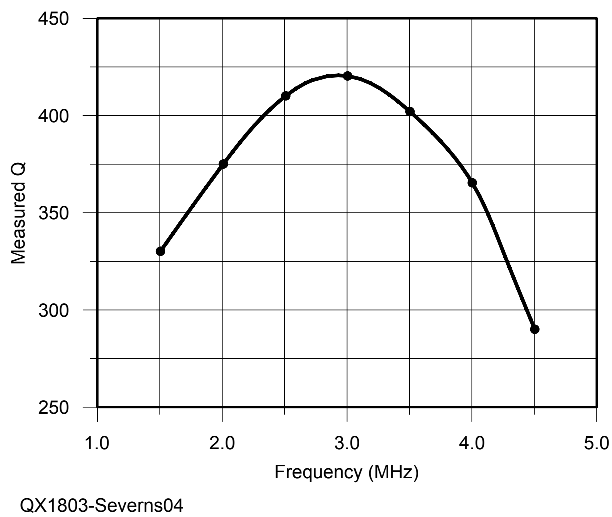

Figure 4 — Q versus frequency for sample R6.

antenna is shortened from 262.4 to 259.6 ft to restore the original fr, Ri is further reduced to 70.3 Ω. Adding insulation does effect the feedpoint impedance. The insulation makes the wire electrically a little longer (≈1.5%).

Now let's suppose we have a buried dipole or a radial system. Burial in soil reduces the resonant frequency drastically so for this example we'll use a dipole length of 30 ft, a burial depth of 1 ft and average soil, $\sigma = 0.005$ S/m and $\varepsilon_r = 13$. Figure 5 shows the behavior of the of the feedpoint impedance (|Zi|) versus frequency as a function of insulation thickness ("A" in inches) varying from zero (bare wire) to 0.020 inches. Clearly the presence of insulation and it's thickness have a profound impact on |Zi| and fr.

The current distribution along the buried dipole is shown in Figure 6. The upper curve is with insulation and the lower is for bare wire.

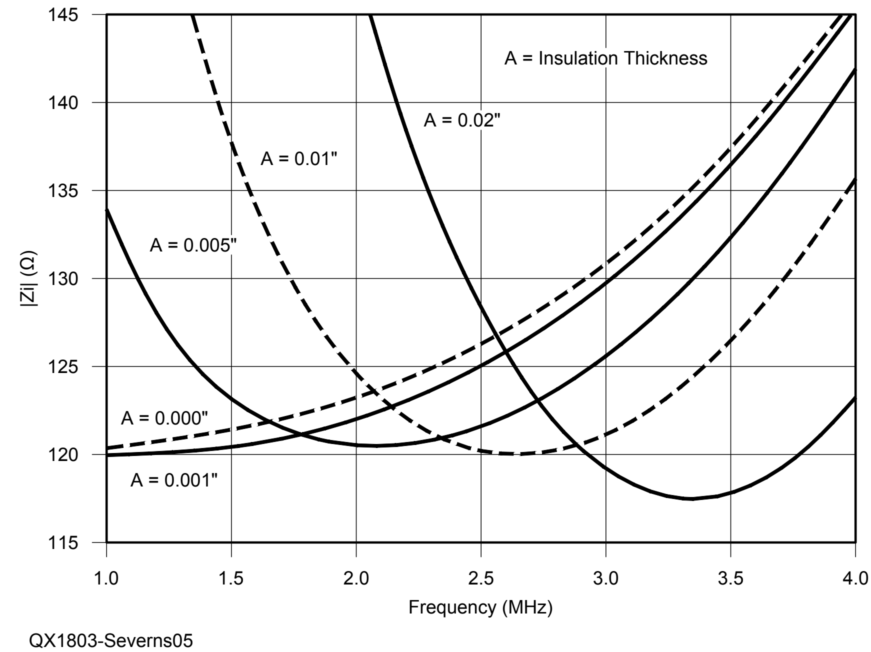

Figure 5 — Magnitude of the feedpoint impedance.

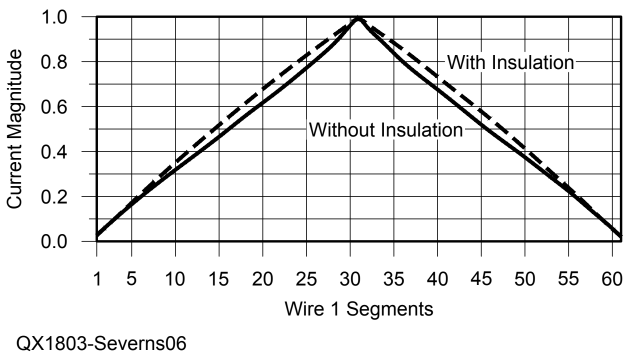

Figure 6 — Current distribution along the dipole with and without insulation.

Verticals with Elevated Ground Systems

Now let's look at the effect of changing from bare to insulated radials in a ground-plane vertical (GPV) like that shown in Figure 7. The vertical and all the radials are #12 AWG wire.

Typically the radials will be wire but the vertical may be either wire or tubing. Tubing is typically not insulated so in this example I looked at three cases: all bare wire, all insulated wire and insulated radials only. In Table 4 the length of the vertical (wire 1) was constant at 134 feet; $\varepsilon_r = 3.3$ for the insulation and perfect ground was assumed.

When the vertical and the radials are bare fr = 1.83 MHz. Adding insulation to the vertical and the radials decreases fr = 1.802 MHz, essentially the same as for the free space dipole. With insulated wire, when the radials are shortened to re-resonate the antenna, Ri increases. However, fr drops much less (to 1.825 MHz) when only the radials are insulated. The same modeling was repeated placing the antenna over real ground. Ri increased to reflect ground losses but the shift in Ri with and without insulation was nearly the same.

When the number of radials was increased to 8, the frequency shift between bare and insulated radials (vertical un-insulated) was only -3 kHz and increasing the number of radials reduced the effect of radial insulation even more. At least for a symmetric radial system with the antenna resonant, insulation appears to have little impact.

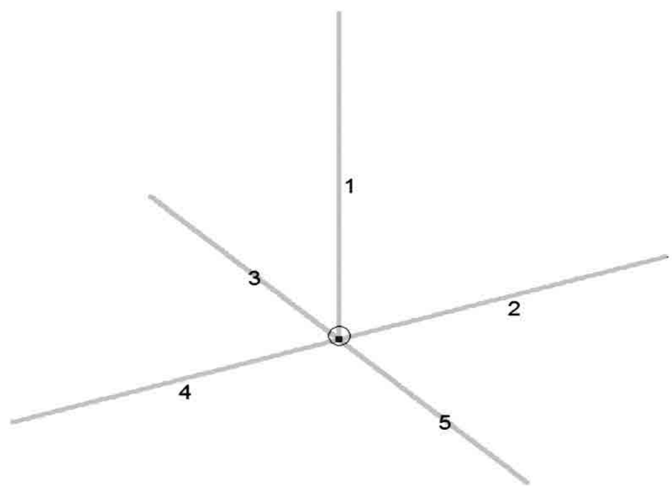

Figure 7 — NEC rendition of GPV with 4 radials.

Radial Length Effects

When the antenna is not ideal, i.e., the radials are too long or the radials are not all the same length, there can be asymmetric

Table 4
Dimensions and impedances with and without insulation.

vertical	*radials*	*f, MHz*	*radial length, ft*	*Ri, Ω*	*Xi, Ω*
bare	bare	1.830	127.6	37.1	0
insulated	insulated	1.830	127.6	37.9	+17.2
insulated	insulated	1.802	127.6	36.1	0
insulated	insulated	1.830	115.7	37.8	0
bare	insulated	1.830	127.6	37.2	+3.2
bare	insulated	1.825	127.6	36.9	0
bare	insulated	1.830	125.4	37.2	0

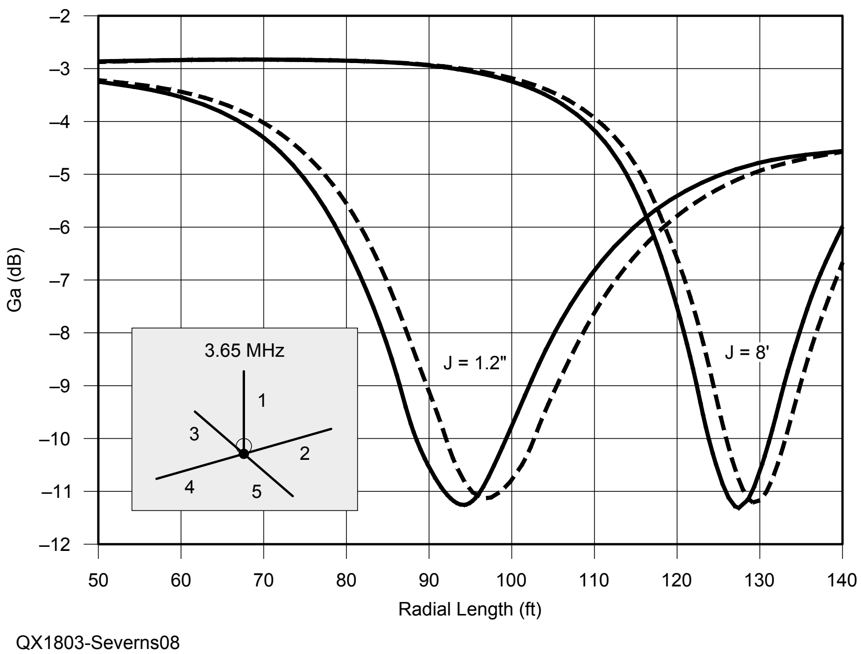

Figure 8 — Average Gain (Ga) for a GP with the base at 1.2 inches, and at 8 feet.

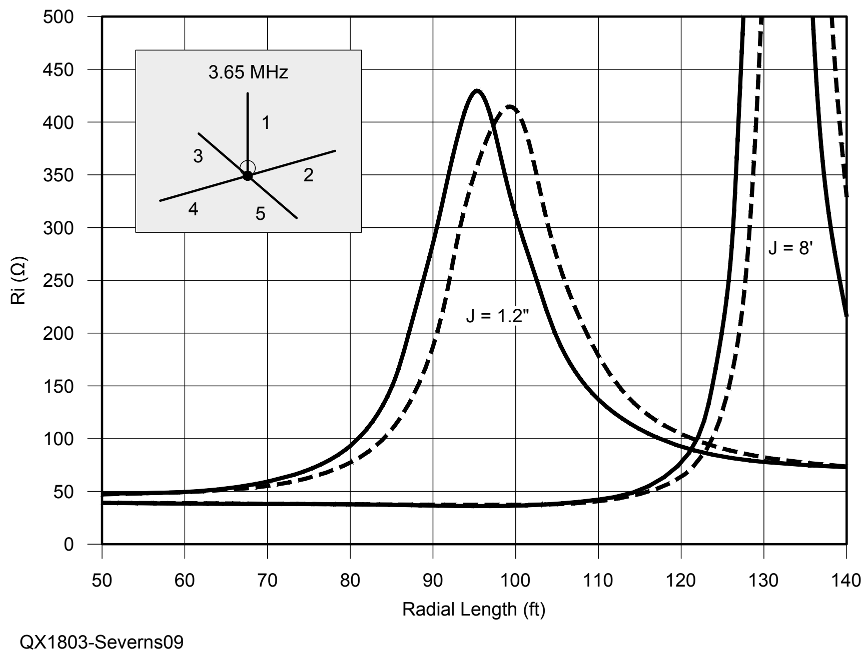

Figure 9 — Ri for a GP with the base at 1.2 inches and 8 feet.

currents on the radials and insulation may not be so benign. My Mar/Apr and May/Jun 2012 *QEX* article[6] on elevated ground systems showed that in some cases there can be a large increase in loss when the radials are asymmetric or too long.

Figure 8 shows the average gain (Ga) of the Figure 7 antenna as the radial length is varied. The height was held constant while the radial length was varied. The height of the antenna above ground (J) was varied from 8 feet down to 1.2 inches over average soil (ε_r = 13, σ = 0.005 S/m). The vertical conductor was not insulated. The dashed lines represent bare wire radials and the solid lines insulated wire radials. The effect of overly long radials can be dramatic (-8 dB) when the radials are well elevated but that's a very unrealistic condition and not likely to be encountered in practice. However, when the radials are lying on the ground even quite normal radial lengths (65-75 ft) can introduce unexpected loss, which is worse with insulation. Figure 9 shows the effect on Ri as the radials are made longer but the scale makes it difficult to really see what's going on with radial lengths of practical interest. Figure 10 has an expanded scale version of the 1.2 inch base height data in Figure 9. We can see that for radials lying on the ground surface it is possible to have a significant increase in Ri with insulation, which should show up with a measurement of feedpoint impedance. It should be pointed out however, that this effect is reduced when more radials are added. Experimental verification of this was shown in Figure 2 of my *QST*[7] and Figures 3 and 4 of my *QEX*[8] articles.

Radial Asymmetry

Besides the effect of radial length, GP antennas with sparse radial systems are very susceptible to asymmetries in radial length which can lead to significant increases in Ri and signal loss. As Dick Weber, K5IU, has shown[9], these effects occur in actual antennas. In an elevated system, radial current asymmetry can be introduced by differences in radial length, nearby conductors, or even lateral variations in ground electrical characteristics under the radial system. For this discussion we'll look at the case with a difference in length between radials. The following graphs assume the radial system is elevated 8 ft over average ground (13, 0.005). The vertical is not insulated and has a constant length of 34 ft. The insulation is assumed to be THHN (ε_r = 3.3) and copper losses are included in the model. In the symmetric case the radial lengths are all 34.1 ft. For the asymmetric case, two radials are 33.1 ft and the other two are 35.1 ft long. Figure 11 is a graph of the feedpoint impedance, Xi versus Ri. For the

Table 5
Vertical with buried radials.

radials	*f, MHz*	*vertical height, ft*	*Ri, Ω*	*Xi, Ω*	*Ga, dB*
bare	1.830	129.0162	49.57	0.00	-5.16
insulated	1.830	129.0162	48.74	-2.44	-5.09
insulated	1.835	129.0162	49.07	0.00	-5.09
insulated	1.830	129.363	49.06	0.00	-5.08

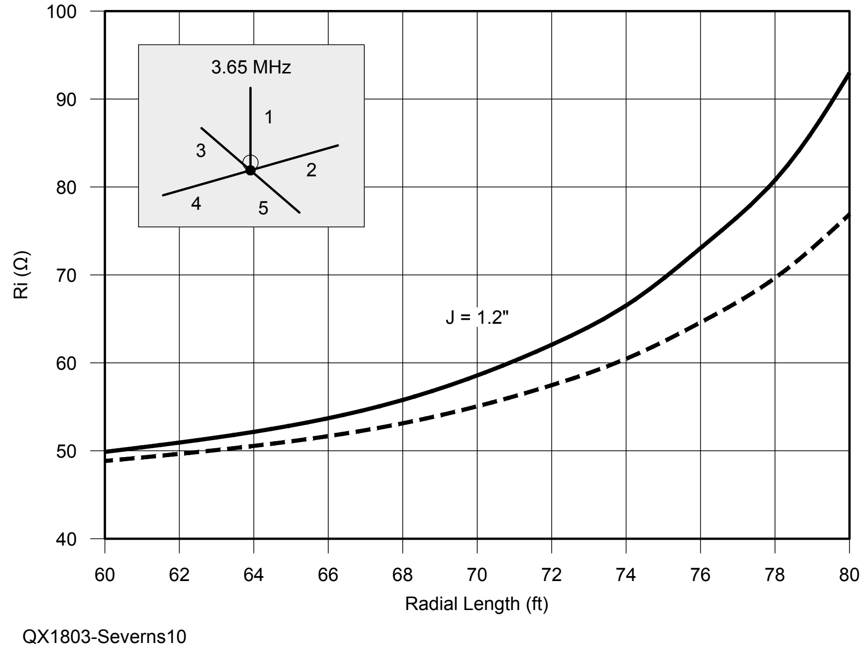

Figure 10 — Ri versus radial length for a GP with the base, and at 1.2 inches.

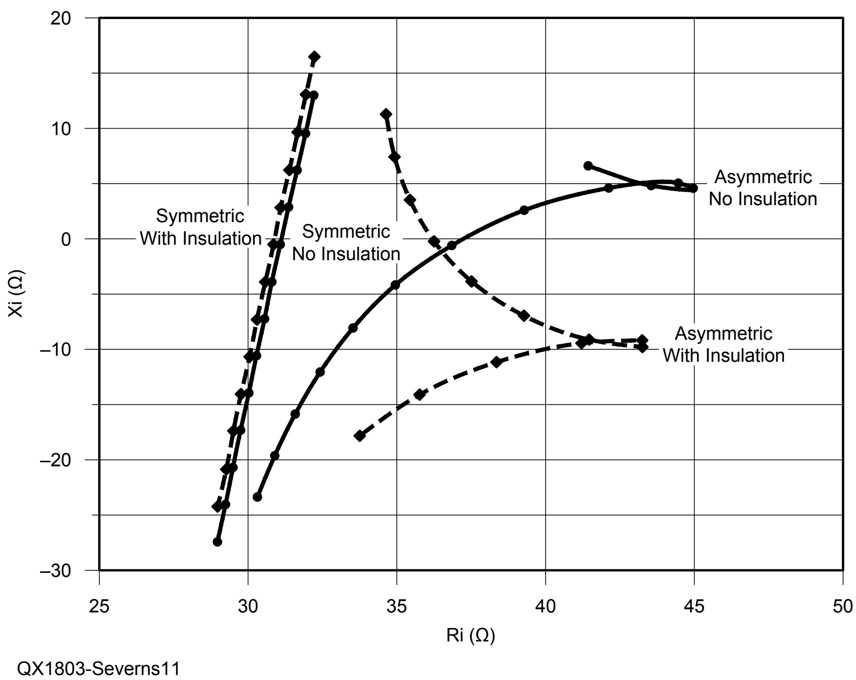

Figure 11 — Feedpoint Xi versus Ri.

symmetric case adding insulation has very little effect but for the asymmetric case the addition of insulation makes a significant difference.

We can look closer at the variation of Ri by graphing Ri versus frequency as shown in Figures 12 and 13. Both with and without insulation Ri can be substantially larger than the symmetric case. The effect of insulation is to shift the plot lower in frequency but the effect is still much the same. In this example there can be up to ±10 Ω difference. If you choose a single frequency to measure Ri the change between not insulated and insulated would depend on what frequency you chose. At 7.10 MHz adding insulation significantly increases Ri but at 7.25 MHz, adding insulation significantly reduces Ri. Confusing! That raises the question of "how much of the Ri increase is due to higher losses?" We can explore that with graphs for average gain (Ga) which show the total loss including ground losses and far-field losses. However, the far-field losses are constant so the differences in Ga will reflect changes in copper and soil loss near the antenna. Ga versus frequency is graphed in Figures 14 and 15. These figures show that the increase in Ri is associated directly with a loss in radiated signal.

The reason for the increase in loss can be seen in the radial currents shown in Figures 16, 17 and 18. In the case of symmetric radials, for I_0 = 1 A, each radial has 0.25 A of current at the inner end tapering off approximately as the cosine of radius. The radial currents are all in phase with the base current I_0. However, in Fgures 17 and 18 we see that the current distribution is asymmetric. More importantly the radial currents are well above 0.25 A. Given that I_0 = 1 A, this looks like a violation of Kirchhoff's law which requires the sum of the currents at a node to add up to zero. What's happening in this case is that the currents are not in-phase, however, the vector sum of the currents is zero. These much higher radial currents are the source of the additional losses.

The dashed lines in Figure 17 and 18 are for 7.0 MHz. The frequencies for the solid lines are labelled in the figures. The asymmetry in the radial currents varies as we move across the band.

Verticals with Buried Radials

Eight buried radials is about the smallest number of practical use. Figure 19 gives an example. The radials are #12 AWG wire 135 ft long, buried 1 ft. The height of the vertical was adjusted to resonate the antenna. Table 5 summarizes the modeling results.

The current distribution along a radial is shown in Figure 20. The solid line is for the bare wire and the dashed line represents

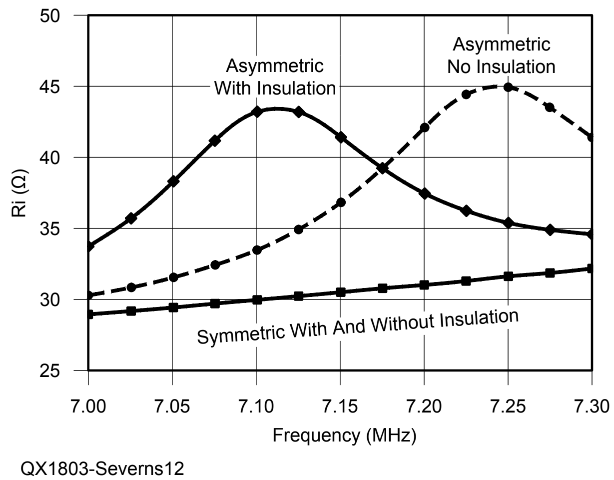

Figure 12 — Feedpoint Ri versus frequency.

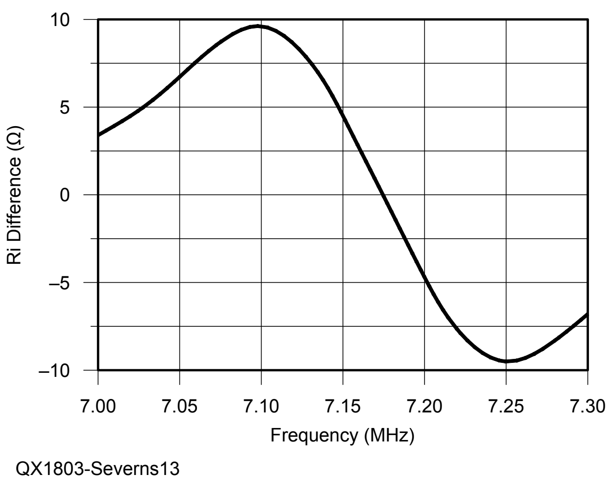

Figure 13 — Ri difference with insulated radials. There is no variation for radials without insulation.

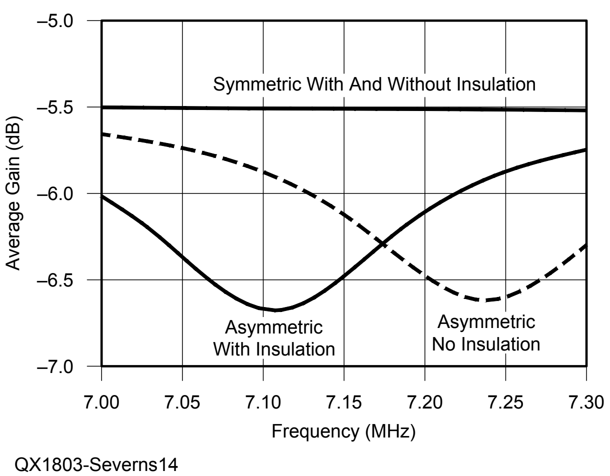

Figure 14 — Average gain (Ga).

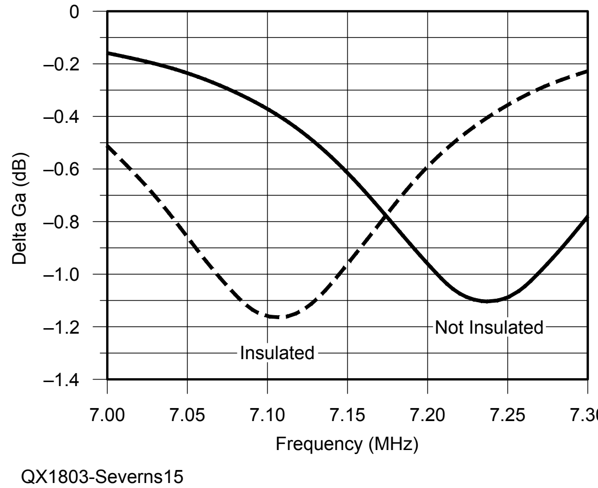

Figure 15 — Ga differences between symmetric and asymmetric radial systems.

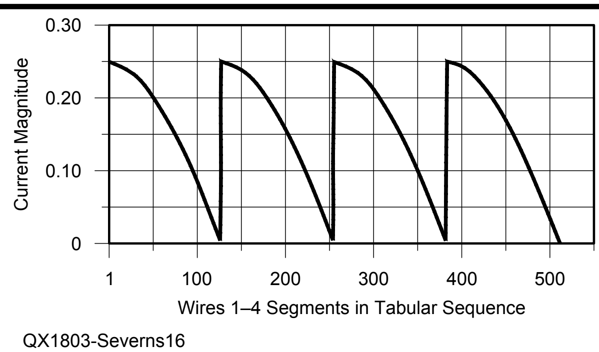

Figure 16 — Radial currents with symmetric radials, no insulation.

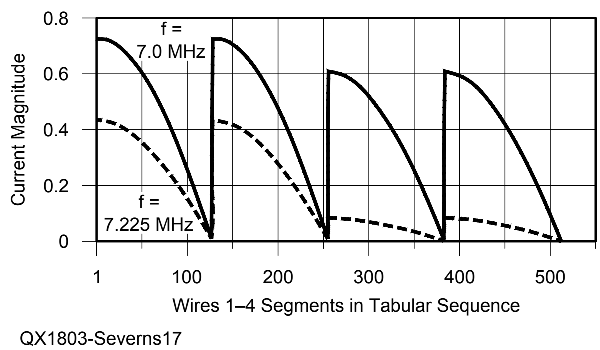

Figure 17 — Radial currents with asymmetric radials, no insulation.

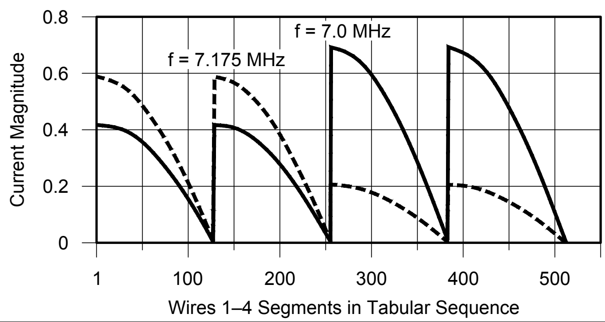

Figure 18 — Radial currents with asymmetric radials, with insulation.

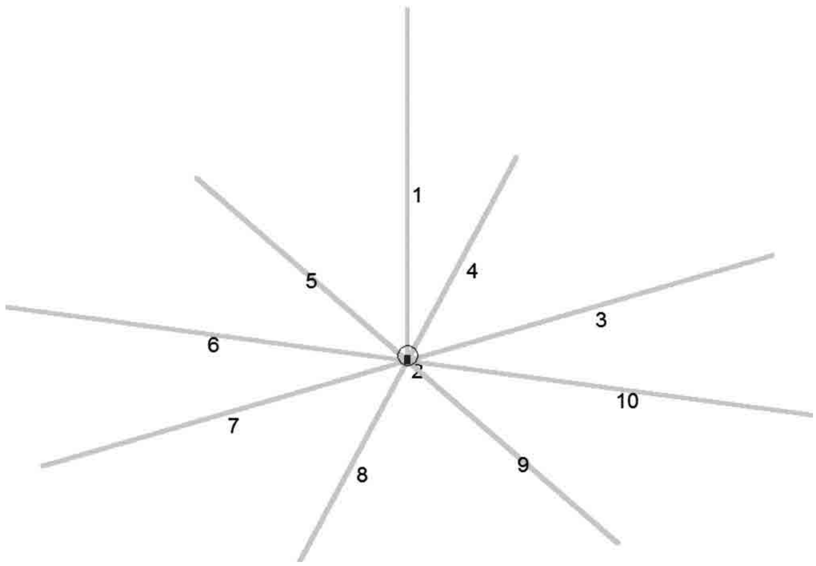

Figure 19 — 160 m vertical with buried radial system.

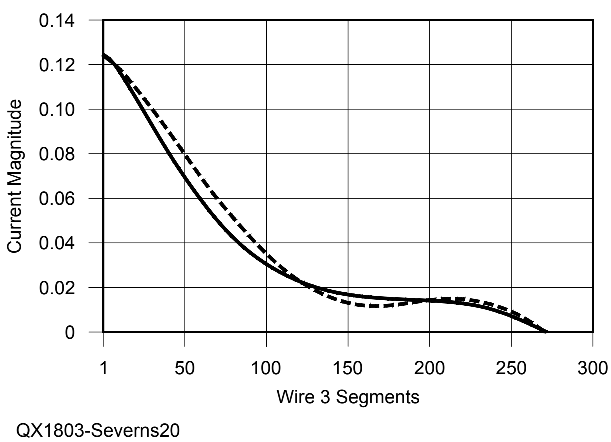

Figure 20 — Radial current distribution.

insulated wire. In this example the resonant frequency increases by 5 kHz as opposed to the decrease we had seen for the dipole and GPV. The effect of insulation on Ri and Ga is very small. There appears to be no reason not to use insulated radials in a buried system.

Mechanical Issues

Leaving the insulation on the wire increases the weight of the wire. If there is icing, the increased diameter could lead to even more weight. From a corrosion point of view insulated radials are very likely to last longer than bare radials, especially for ground surface or buried radials.

Conclusions

From this work it seems that leaving the insulation on the wire is generally benign and loss due to the insulation, either new or old, does not seem to be significant. However, it was shown that in certain cases, mostly related to GP-verticals with sparse radial systems there can be a substantial impact. However, that really occurs only when very few radials are used. These problems tend to go away as the radial count is increased to twelve or more for elevated radials and 16-20 for ground surface or buried radials.

Rudy Severns, N6LF, was first licensed as WN7WAG in 1954. He is a retired electrical engineer, an IEEE Fellow and ARRL Life Member.

Notes

[1]R. Severns, N6LF, "Conductors for HF Antennas", *QEX*, Nov./Dec., 2000, pp. 20-29.
[2]R. Severns, N6LF, "Tech Notes", *QEX*, May/June 2002, pp. 55-56.
[3]R. Lewallen, Roy, W7EL, EZNEC Pro/4 v6, **www.w7el.com**.
[4]D. Maguire, AC6LA, AutoEZ, **ac6la.com/autoez.html**.
[5]Rudy Severns, N6LF, "The Case of the Declining Beverage-on-Ground Performance", *QEX*, Jul./Aug., 2016, pp. 7-18.
[6]Rudy Severns, N6LF, "A Closer Look at Vertical Antennas With Elevated Ground Systems", *QEX*, Mar./Apr., and May./Jun., 2012.
[7]R. Severns, N6LF, "An Experimental Look at Ground Systems for HF Verticals", *QST*, Mar., 2010, pg. 30
[8]R. Severns, N6LF, "Experimental Determination of Ground System Performance - Part 2", *QEX*, Jan./Feb., 2009, pp. 48-52.
[9]D. Weber, K5IU, "Optimum Elevated Radial Vertical Antennas", *Communications Quarterly*, Spring 1997, pp. 9 – 27.

Increase Your Resistor Inventory with this Resistor Search Program

The average hobbyist might own a few resistor kits, but if you don't want to own every resistance value or are in a hurry to breadboard something and you need an exact resistance value, you can combine resistors to make up what you need. But who wants to search through all their resistors every time then calculate the required value from what's on hand, or worse yet to just get within 10 or 20%. The key is knowing what's on hand. You can figure it all out ahead of time by applying my ReSearch program.

The Key is Organizing a List

In my approach you select certain combinations of resistors in parallel, calculate those combinations and list the results. Since it doesn't help much to combine very large values with very small ones (say, one megohm with one ohm) the values selected should be closer together. Applying this principle, I chose sets of increasing value resistors, with the first in the set (lowest value), paired consecutively with each of the next higher values on the list. I did this for the entire range of my resistors. Each set yields n = 2 + (the number of consecutive resistors values). The program thus produces a list of resistance values several times greater than the list of actual owned resistors.

The key is making and keeping an up-to-date list of all the resistor values that you have on hand. I have a few kits containing a total of 51 values, and it took me less than 10 minutes to create the list in a text file. So, for just a little up front (and on-going) effort I now have a list of about 600 resistance values to choose from. To make a desired resistance, it is necessary only to choose the values from the new list and combine them.

MatLab Code and Resistor Lists

I generated and ran the code in MatLab, but it can be adapted to C or other languages. The actual code is available on the **www.arrl.org/qexfiles** web page. The program input format is a one-column list of resistor values in a text file. Engineering, scientific, integer or decimal format can be used in MatLab, as seen in the Table 1 example of 12 values.

Normally I search to a depth of 10, which in this case would yield 89 values, but for this shorter illustration, the search depth is 3. This example input (Table 1) yielded the 54 computed values (Table 2) with a search depth of 3:

For each computed set, the output list includes each owned resistor, the owned resistor paralleled with itself, and the 3 successive resistor parallel combinations. Each row of the output list contains from left to right: the combined value, selected resistor #1, and selected resistor #2. Resistor #1 and resistor #2 are zero in rows containing the owned resistor.

Table 1.
An example of 12 values input to the *ReSearch* program from file "inputReslistPublish.txt".

#	*Resistance, Ω*
1	1.6
2	3
3	50.2
4	170
5	4.7E+02
6	1000
7	2E+03
8	2.2E+03
9	5000
10	6700
11	1.2E+04
12	1.2E+06

Table 2.
List of computed values with a search depth of three.

#	*Computed Resistance*	*Owned Resistor#1*	*Owned Resistor#2*	*#*	*Computed Resistance*	*Owned Resistor#1*	*Owned Resistor#2*
1	8.0000e-01	1.6000e+00	1.6000e+00	28	6.8750e+02	1.0000e+03	2.2000e+03
2	1.0435e+00	1.6000e+00	3.0000e+00	29	8.3333e+02	1.0000e+03	5.0000e+03
3	1.5000e+00	3.0000e+00	3.0000e+00	30	1.0000e+03	0	0
4	1.5506e+00	1.6000e+00	5.0200e+01	31	1.0000e+03	2.0000e+03	2.0000e+03
5	1.5851e+00	1.6000e+00	1.7000e+02	32	1.0476e+03	2.0000e+03	2.2000e+03
6	1.6000e+00	0	0	33	1.1000e+03	2.2000e+03	2.2000e+03
7	2.8308e+00	3.0000e+00	5.0200e+01	34	1.4286e+03	2.0000e+03	5.0000e+03
8	2.9480e+00	3.0000e+00	1.7000e+02	35	1.5278e+03	2.2000e+03	5.0000e+03
9	2.9810e+00	3.0000e+00	4.7000e+02	36	1.5402e+03	2.0000e+03	6.7000e+03
10	3.0000e+00	0	0	37	1.6562e+03	2.2000e+03	6.7000e+03
11	2.5100e+01	5.0200e+01	5.0200e+01	38	1.8592e+03	2.2000e+03	1.2000e+04
12	3.8756e+01	5.0200e+01	1.7000e+02	39	2.0000e+03	0	0
13	4.5356e+01	5.0200e+01	4.7000e+02	40	2.2000e+03	0	0
14	4.7800e+01	5.0200e+01	1.0000e+03	41	2.5000e+03	5.0000e+03	5.0000e+03
15	5.0200e+01	0	0	42	2.8632e+03	5.0000e+03	6.7000e+03
16	8.5000e+01	1.7000e+02	1.7000e+02	43	3.3500e+03	6.7000e+03	6.7000e+03
17	1.2484e+02	1.7000e+02	4.7000e+02	44	3.5294e+03	5.0000e+03	1.2000e+04
18	1.4530e+02	1.7000e+02	1.0000e+03	45	4.2995e+03	6.7000e+03	1.2000e+04
19	1.5668e+02	1.7000e+02	2.0000e+03	46	4.9793e+03	5.0000e+03	1.2000e+06
20	1.7000e+02	0	0	47	5.0000e+03	0	0
21	2.3500e+02	4.7000e+02	4.7000e+02	48	6.0000e+03	1.2000e+04	1.2000e+04
22	3.1973e+02	4.7000e+02	1.0000e+03	49	6.6628e+03	6.7000e+03	1.2000e+06
23	3.8057e+02	4.7000e+02	2.0000e+03	50	6.7000e+03	0	0
24	3.8727e+02	4.7000e+02	2.2000e+03	51	1.1881e+04	1.2000e+04	1.2000e+06
25	4.7000e+02	0	0	52	1.2000e+04	0	0
26	5.0000e+02	1.0000e+03	1.0000e+03	53	6.0000e+05	1.2000e+06	1.2000e+06
27	6.6667e+02	1.0000e+03	2.0000e+03	54	1.2000e+06	0	0

With a search depth of 10 we can increase our choice of resistance by a factor of 7. In this case, a search depth of 3 yielded a factor of more than 4.

The program can also add up the series resistance values to form the required resistance. For example, If a value of 1234 Ω is requested, the program will choose the combination of resistances, #33, #17 and #10 twice from the Table 3 to form a resistance of 1,230.8 Ω, which is less than 0.3% different from the requested value (see the program output in Table 2). For this mix of owned resistors the same result is also attainable with only a search depth of 2.

This is only one of a *large* number of possible algorithms to conduct a search. Some alternatives would be changing the search depth, or the set selection process or the number of parallel resistances. Development is ongoing. So check back for updates. — *Dan Bobczynski, KG4HNS, kg4hns@gmail.com*.

Quadrature Direction Finding

Using quadrature techniques we can extract more complete information about a distant signal, and thus more easily determine its direction. Translate the signals received from three omnidirectional antennas to baseband with the same local quadrature oscillator. Then low-pass filter them and numerically deduce the azimuth of the emitting signal from the resulting six dc voltages.

This quadrature approach shares aspects of the three standard techniques[1, 2] — Watson-Watt, pseudo-Doppler, and phase interferometry — of stationary antenna direction finding.

The physical apparatus

The goal is to discover the azimuth of an incoming plane wave from a distant emitter. Place three identical omnidirectional receiving antennas at *O* (origin), *E* (east), and *N* (north), where *E* and *N* are points at the 0- and 90-degree positions respectively on the circumference of a circle of radius *d* centered at the center *O* as in Figure 1. The radius *d* must be less than λ/2, where λ is the wavelength of the signal. Connect the three antennas using three transmission lines of identical electrical lengths to a three-input receiver. Within this receiver

Table 3.

======	**MatLab Output**	**======**
ReSearch Resistor list file name ?	/inputReslistPublish.txt	
Search depth ?	(0 ends program)	3
Desired resistance ?		1234
Desired resistance, percent % tolerance ?		0.3
Use_these_ncsorted_resistances	=	
	1.1000e+003	
	124.8438e+000	
	3.0000e+000	
	3.0000e+000	
To_obtain_this_resistance	=	1.2308e+003
Actual_Tolerance	=	0.25577
ncsorted	=	
8.0000e-01	1.6000e+00	1.6000e+00
1.0435e+00	1.6000e+00	3.0000e+00
1.5000e+00	3.0000e+00	3.0000e+00
1.5506e+00	1.6000e+00	5.0200e+01
1.5851e+	1.6000e+00	1.7000e+02
1.6000e+00	0	0
2.8308e+00	3.0000e+00	5.0200e+01
2.9480e+00	3.0000e+00	1.7000e+02
2.9810e+00	3.0000e+00	4.7000e+02
3.0000e+00	0	0
2.5100e+01	5.0200e+01	5.0200e+01
3.8756e+01	5.0200e+01	1.7000e+02
4.5356e+01	5.0200e+01	4.7000e+02
4.7800e+01	5.0200e+01	1.0000e+03
5.0200e+01	0	0
8.5000e+01	1.7000e+02	1.7000e+02
1.2484e+02	1.7000e+02	4.7000e+02
1.4530e+02	1.7000e+02	1.0000e+03
1.5668e+02	1.7000e+02	2.0000e+03
1.7000e+02	0	0
2.3500e+02	4.7000e+02	4.7000e+02
3.1973e+02	4.7000e+02	1.0000e+03
3.8057e+02	4.7000e+02	2.0000e+03
3.8727e+02	4.7000e+02	2.2000e+03
4.7000e+02	0	0
5.0000e+02	1.0000e+03	1.0000e+03
6.6667e+02	1.0000e+03	2.0000e+03
6.8750e+02	1.0000e+03	2.2000e+03
8.3333e+02	1.0000e+03	5.0000e+03
1.0000e+03	0	0
1.0000e+03	2.0000e+03	2.0000e+03
1.0476e+03	2.0000e+03	2.2000e+03
1.1000e+03	2.2000e+03	2.2000e+03
1.4286e+03	2.0000e+03	5.0000e+03
1.5278e+03	2.2000e+03	5.0000e+03
1.5402e+03	2.0000e+03	6.7000e+03
1.6562e+03	2.2000e+03	6.7000e+03
1.8592e+03	2.2000e+03	1.2000e+04
2.0000e+03	0	0
2.2000e+03	0	0
2.5000e+03	5.0000e+03	5.0000e+03
2.8632e+03	5.0000e+03	6.7000e+03
3.3500e+03	6.7000e+03	6.7000e+03
3.5294e+03	5.0000e+03	1.2000e+04
4.2995e+03	6.7000e+03	1.2000e+04
4.9793e+03	5.0000e+03	1.2000e+06
5.0000e+03	0	0
6.0000e+03	1.2000e+04	1.2000e+04
6.6628e+03	6.7000e+03	1.2000e+06
6.7000e+03	0	0
1.1881e+04	1.2000e+04	1.2000e+06
1.2000e+04	0	0
6.0000e+05	1.2000e+06	1.2000e+06
1.2000e+06	0	0
======	**End of MatLab Output**	**======**

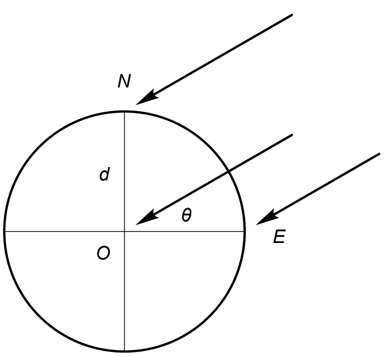

QX1801-MacCluer01

Figure 1 — Three omnidirectional antennas are placed at points *O*, *N*, and *E*, where *O* is the center of a circle of radius *d* < λ/2, and where λ is the wavelength of a distant emitter signal that is arriving at polar angle θ.

mix our three samples of frequency $f = \omega/2\pi$ (of wavelength λ) with a local quadrature signal at the emitter frequency f to obtain six low-pass filtered dc voltages, where v_0 and v_{90} of Figure 2 are: o_0, o_{90}, e_0, e_{90}, n_0, n_{90}. for the three quadrature circuits. The azimuth of the emitter can now be mathematically deduced as follows.

Lead times of the received signals

Referring to Figure 1, the plane wave arrives at point E exactly at time τ_E seconds before arriving at the center O,

$$\tau_E = \frac{d}{c}\cos\theta \qquad (1a)$$

where d is the radius of the circle and c is the speed of light. Likewise, the plane wave arrives at N exactly

$$\tau_E = \frac{d}{c}\sin\theta \qquad (1b)$$

seconds before arriving at O.

$$\frac{1}{2}\left[\cos(2\omega t + \omega\tau + \beta) + \cos(\omega t - \beta)\right]$$

which, when passed through a low-pass filter, yields (within a known amplitude) the dc voltage

$$v(\tau, \beta) = \cos(\omega\tau - \beta)\,. \qquad (2)$$

The six baseband dc voltages

Specialize Eq(2) to each antenna signal voltage in turn and deduce the azimuth.

Step 1: Apply quadrature mixing to the antenna voltage at the center O,

$$v(0, \beta) = \cos(-\varphi) = \cos(\varphi) \qquad (3a)$$

and

$$v(0, \varphi + \frac{\pi}{2}) = \cos(-\varphi - \frac{\pi}{2}) = -\sin(\varphi) \qquad (3b)$$

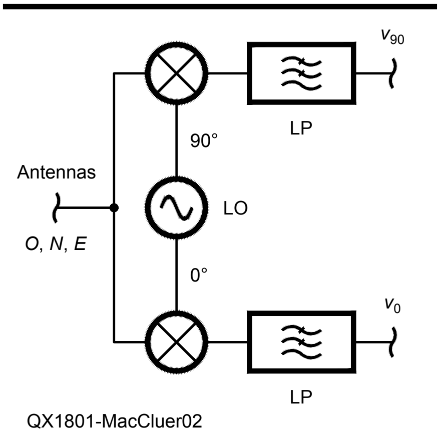

Figure 2 — Each of the three omnidirectional antenna signals are quadrature-mixed by the same local oscillator and low-pass filtered to dc.

where $-\pi < \varphi \le \pi$ is the angle at which the emitter signal lags the local I-channel at O. After normalizing, by consulting a trigonometric lookup table, we can obtain from Eq(3a) and (3b) the phase lag angle φ, rather than resorting to electronically phase locking the local oscillator to the emitter.

Step 2: From Eq(1a), the E-antenna signal is mixed with the base-band quadrature LO signal resulting in two dc voltages,

$$e_0 = v(\tau_E, \varphi) = \cos\left(\frac{\omega d\cos\theta}{c} - \varphi\right) \qquad (4a)$$

and

$$e_{90} = v(\tau_E, \varphi + \frac{\pi}{2}) = \cos\left(\frac{\omega d\cos\theta}{c} - \frac{\pi}{2} - \varphi\right) = \sin\left(\frac{\omega d\cos\theta}{c} - \varphi\right) \qquad (4b)$$

From (4a) and (4b) we can obtain (within a multiple of 2π) the value of

$$\left(\frac{\omega d\cos\theta}{c} - \varphi\right)$$

Adding the computed value φ from Eq(3), we find the angle between $-\pi$ and $+\pi$ that differs by an integral multiple of 2π from our sought-for value $(\omega d/c)\cos\theta$. To guarantee that we have obtained its actual value rather than its equivalent angle modulo 2π, we impose a critical assumption.

Geometric anti-aliasing

The radius d of the circle of Figure 1 must be less than half the wavelength λ. As a consequence, because $\omega\lambda = 2\pi c$, the crucial inner term of Eq(4a) and (4b) satisfies

$$-\pi < \frac{\omega d\cos(\theta)}{c} < \pi$$

and thus we have already obtained the actual numerical value

$$A = \frac{\omega d\cos(\theta)}{c}\,. \qquad (5)$$

Step 3: Quadrature mixing the N-antenna signal down to baseband yields

$$n_0 = v(\tau_N, \varphi) = \cos\left(\frac{\omega d\sin\theta}{c} - \varphi\right) \qquad (6a)$$

and

$$n_{90} = v(\tau_N, \varphi + \frac{\pi}{2}) = \cos\left(\frac{\omega d\sin\theta}{c} - \frac{\pi}{2} - \varphi\right) = \sin\left(\frac{\omega d\sin\theta}{c} - \varphi\right) \qquad (6b)$$

Adding in φ modulo 2π to the inner terms of, (6a) and (6b) will yield

$$B = \frac{\omega d\sin(\theta)}{c}\,. \qquad (7)$$

Step 4: By normalizing A and B, we obtain from Eq(5) and (7) the polar angle θ, and hence the azimuth angle is

$$AZ = \frac{\pi}{2} - \theta \text{ radians.} \qquad (8)$$

Suggested implementation

A simple prototype receiver could be built with three signal splitters, followed by six passive double-balanced mixers, all driven by a shared quadrature LO. The LO can be a DDS running at four times the emitter frequency followed by a divide-by-four to obtain the 0- and 90-degree shifts. The six resulting IF signals could be low-pass filtered by a simple series radio frequency choke with a small shunt capacitor. Then boost the signal by six identical op-amps. The op-amp power supply must be balanced about signal ground since we are acquiring dc voltages.

Assuming the emitter is fixed or at least not in rapid motion, the six resulting dc voltages are varying at propagation-fading rates. Even a simple Arduino could sample the six dc voltages on six separate analog ports in a sufficiently rapid rotation to obtain six accurate, more-or-less simultaneous samples (that may need to be individually averaged). The Arduino could perform the four successive quadrature inversions by lookup-table interpolation, or by an arctangent/sign-disambiguation subroutine. A second Arduino could then display the computed azimuth on a LCD shield.

Your challenge

I have provided an apparently simple approach to direction finding. It is a mathematical observation that requires proof of concept. Your challenge is to implement and inform the community of your results. — *Best regards, Chuck MacCluer, W8MQW, w8mqw@arrl.net.*

Notes

[1]W. Reed, "Review of conventional tactical radio direction finding systems", Defence Research Establishment Ottawa, Tech. Note 89-12, May, 1999, **www.dtic.mil/dtic/tr/fulltext/u2/a212747.pdf**.

[2]Rohde & Schwarz. "Introduction into the theory of radio direction finding", Radiomonitoring & Radiolocation, Catalog 2011/2012, **www.telekomunikacije.etf.bg.ac.rs/predmeti/ot3tm2/nastava/df.pdf**.

Letters

Automatic Tracking Filter for DDS Generator (Jul/Aug 2017)

Dear Editor,

I simulated the circuit for the 20 MHz filter in the Riccardo Gionetti, IØFDH, article using LTSpice. My curve (Figure A) does not match the curve shown in Figure 10 of the article.

There isn't enough information in the article about the two transformers to allow me to prepare a precise circuit for the simulation. The inductance is given, but the turns ratio is not given, and it is not stated which winding the inductance is for, so I assumed it was for the larger winding. Also, the coupling coefficient is not given, so I tried several values to see if I could get reasonable results. Another concern is that the curve in Figure 10 shows notches on each side of the resonant peak, which are not present in my simulation. Also the response above resonance for my simulation just tails off at high frequencies. The response in Figure 10 looks similar to that of an elliptical filter. I used ideal inductors to simulate the transformers, so the Q of the inductors was not a factor. I used RB510SM-30 diodes, which are specified at 100 mA, 30 V and 6 pF at 0 V because there was no LTSpice model available for the BAT46 used in the article.

I would like to know what are the causes of the disparities I observed in my simulation relative to that of the article? I would also like to know enough about the transformers so that I could duplicate them, or make a good approximation of them.

The design is clever, interesting, and potentially useful for me. I would like to understand it better so I could simulate it well and possibly use it in an application I have in mind. — *Regards, Jim McLucas, KCØVDC.*

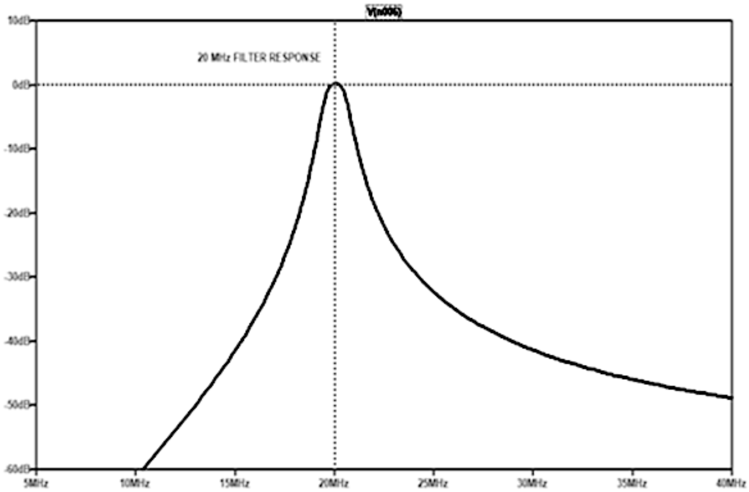

Figure A — Simulated response of 20 MHz filter.

[The author replies]

In response to Jim's two questions: first, the transformer coils I used in my prototype are miniature 10 mm package very similar to Coilcraft "Slot Ten" style shown in Figure B. The winding detail is shown in Figure C for one of the transformer coils. The Q using a Boonton Q-meter is 110 at 15 MHz. The coils are wound using 0.15 mm diameter wire as follows.

L1A, L1B — 10 + 10 turns, link 4 turns.

L2A, L2B — 7 + 7 turns, link 3 turns.

L3A, L3B — 5 + 5 turns, link 3 turns.

L4A, L4B — 3 + 3 turns, link 2 turns.

The difference between the curve shown in my Figure 10 and the curve of Jim's Figure A simulation is that a simulation of only one band pass filter is not exhaustive, since it does not take into account the coupling with the other filters and components, which may exhibit notches or peaks outside the main peak. It is very likely they are due to the switching diodes, that are not perfect switches. Furthermore, there are no screens between the band pass filters in my prototype. — *73, Riccardo Gionetti, IØFDH.*

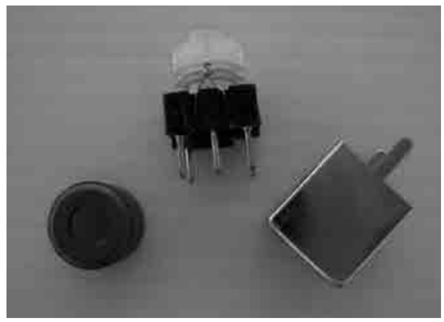

Figure B — Miniature 10 mm transformer package. The winding is made as in Figure C.

Weatherproofing Experiment with PL-259 Connectors (Sep/Oct 2017)

Dear John,

Thanks for an interesting article about weather protection of RF connectors. I have used UHF connectors (PL-259, etc.) extensively since I got my first license in 1971. I have never had problems caused by water entering the connection, or cable, in spite of living most of my life in Finland.

There seems to be something strange about your results with what you call "fusion tape", especially for the "first construction" (Figure 5). You don't describe exactly how you protected the connections and the photo of Figure 2 is not clear enough to see. Did you really put electrical tape under the fusion tape in cables 3 and 4? I have always sealed my outside RF connectors with "fusion tape". It works extremely well and is fairly easy to apply, but has to be done correctly.

First of all, clean the connector surfaces for fingerprints, and so on, with industrial alcohol — isopropanol works well and evaporates quickly. Never put anything under the rubber tape! Whatever is between the rubber and connector body defeats the protection provided by the "fusion tape", because the rubber is not in direct contact with the metal of the connector. Apply the plain fusion tape directly over the connection, at least 2 to 3 cm over the cable and as far over the female connector as physically possible — up to the flange of a bulkhead connector or over the whole barrel and the other cable, if that is possible. Do not leave any part of the connector visible, and use an unbroken length of tape for the entire application. Any exposed metal will corrode in time and may eventually cause water seepage into the connection. Stretch the tape tight without breaking it — it will stretch to about three times the original length. There must be at least two layers of rubber tape over the whole protected area. Of course, this must be done in dry weather with temperature of at least +15 °C. Then, on the next day the tape will have fused into a solid block of rubber. If not, then you used the wrong kind of tape, or the temperature was too cold. When done properly, the tape will be fairly difficult to remove, if the need ever arises. To remove it, cut a lengthwise slit on the tape with an X-Acto or similar knife. Be careful to not spoil the cables or connectors, and peel the rubber off.

My protected connections this way have lasted 20 years in the Finnish weather conditions, with rain, snow, ice, direct sunshine at +30 to -30 °C. I did not use anything else like electrical tape or cable ties over the connections. When I disassembled my antennas prior to moving to Crete, Greece, all connectors under the rubber were still shiny and there was absolutely no indication that water had ever gotten inside. I don't recall the brand of "fusion tape" I used those days. — *73, Jukka Siitari, SV9RMU (also OH2AXE); siitarijukka@gmail.com*.

Dear John,

This is a very interesting article. Electricians have been splicing high and medium voltage cables since just about 1900. Some underground splices last 20 to 50 years. Although the high voltage cable is quite a bit different from coax, some of the elements are similar or identical.

Electricians use many types of tape, but the two of interest are the ones you used. Each is used differently. Vinyl tape is applied with modest tension on the tape and with half width overlap. Synthetic rubber or silicon tape (fusible) is applied with higher tension so that due to stretching the width is halved when applied to the cable, again with half width overlap. The tension causes the tape to fuse without voids. Vinyl tape has the void you so well pointed out, so it can be used for protection, but the fusible tape goes on the bottom! You should follow these guidelines.

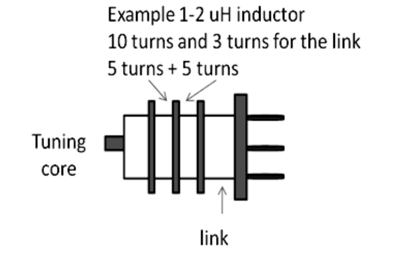

Figure C — Sample winding detail for coils L3A or L3B.

First, clean the cable and connector. The most important part of splicing is cable preparation. Make sure there are no containments, and sand down the insulation to make sure there are no voids or ridges on the insulation. Molding ridges along the length of the cable will cause a void just like you saw with the vinyl tape.

Second, tape any step changes of diameter with vinyl tape to make smooth transitions for the insulating tape layer. Place several layers of half-inch vinyl tape adjacent to any step change in outside diameter. The step at the rear of the connector would take perhaps three layers of tape, each quarter inch shorter than the one beneath. The bottom layer should be one and a half or two inches in length. The smaller steps might require just half an inch of taper. The tape wrap shown in the article with the tape stretched over some large steps would function well only in a dry environment.

Clean the cable one last time with alcohol or acetone. The fusible tape, synthetic rubber or silicone, is applied with enough tension to stretch the tape to half its width. Make the lay very smooth over the small steps in the tapers made with vinyl tape. If you want to protect the fusible tape from abrasion or sun damage, overwrap it with friction tape or vinyl tape.

Vinyl tape can be used for a waterproof wrap if it is over-coated with a liquid vinyl product. Take care to cover the ends of the tape on both ends with the liquid for the reasons you mentioned in the article.— *Richard Myers; dickmyers9@cs.com*.

[The author replies] Hi Jukka and Richard,

Thanks for your comments on weatherproofing coax connections.

Regarding vinyl tape, yes, I had put vinyl tape on as the first layer in most cases. I did this so that when a joint has to be opened for re-routing or repair, I found the surface of the coax and connector may be contaminated with a waterproofing material, particularly in the past where gooey messes were left on the cable and connector.

Both letter writers agree that fusion tape ought to be the first layer to be applied. Also the cable should be cleaned with industrial alcohol (isopropanol or acetone), none of which I used as my cables appeared clean by visual inspection. Cleaning with the mentioned liquids is a good idea, which I will do.

In the application of fusion tape, I did wrap it tightly with 50% overlap but I get the impression that I did not stretch as tightly as recommended by both of you. The writers suggest stretching by either three times the original length, or stretching to halve the width. I can understand that under this amount of tension, the voids would close.

A very positive outcome about writing this article is that one learns something. I like the idea of using the fusion tape over a cleaned cable. Seems like a single really tight wrap is better than the layered approach that I took. However I think I would still put a vinyl wrap on top of the fusion tape for ultra-violet protection. Thank you your comments. — *73, John White, VA7JW*.

Measuring Characteristic Impedance of Coax Cable in the Shack (Nov/Dec 2017)

[Several readers had difficulty finding the out-of-print reference mentioned in the John Flood, K4DLX, Technical Note. The author explains. — *Ed.*]

Dear Editor,

The technique presented in my Technical Note is based on a well-known property of transmission lines (see John D. Kraus, *Electromagnetics*, 1953, pp. 433ff.)". This reference is the same as Table 10-3, John D. Kraus, *Electromagnetics, Third Edition*, 1984, p. 406. The earlier reference is out of print. I am referring to the equation, reproduced below, that appears in the third row and third column of Table 10-3,

$$Z_x = jZ_0 \tan \beta x$$

where $\beta = 2\pi/\lambda$ = phase constant in radians per meter, and where λ is the wavelength. Specifically, when length $x = \lambda/8$, then $\beta x = \pi/4$ (45 degrees), and $|Z_x| = Z_0$. — *Best regards, John Flood, K4DLX; k4dlx@bellsouth.net.*

Send your *QEX* Letters to the Editor to, ARRL, 225 Main St., Newington, CT 06111, or by fax at 860-594-0259, or via e-mail to qex@arrl.org. We reserve the right to edit your letter for clarity, and to fit in the available page space. "Letters to the Editor" may also appear in other ARRL media. The publishers of *QEX* assume no responsibilities for statements made by correspondents.

Upcoming Conferences

16th Annual Southern California Liniux Expo (SCaLE)

Pasadena, California
March 8 – 11, 2018
www.socallinuxexpo.org/scale/16x

The 16th annual Southern California Linux Expo (SCaLE) will be held March 8 – 11, 2018 at the Pasadena Convention Center, Pasadena, California.

SCaLE is unique among computer shows in that they offer event-resources to any Open-source software group that has a good story to tell. As a result, of the 150+ booths on the Exposition floor, about a third aren't trying to sell you anything ... not for money, anyway.

For years, SCaLE has highlighted many specialty areas where technology overlaps with the Linux and Open-source Community. In 2015, SCaLE began hosting annual Amateur Radio representation as well, in the form of: A Special Event radio station (N6S) operating live from PCC, manned by hams from the Ventura County Amateur Radio Society, to answer questions about Amateur Radio and how it relates to Linux and the Open-source community; a specialty booth manned by the Amateur Radio Emergency Data Network, demonstrating and answering questions about the "Ham Mesh Net" project; and a license exam session, Sunday, March 11, open to the public.

In addition, SCaLE invites people to present papers and discussions from all aspects of the user community. This year they began hosting an Amateur Radio related track of speaker sessions; this year's sessions include: Orv Beach, W6BI, "Linux and the Ham Radio 'Internet'"; Dr. Kate Hutton, K6HTN, "Amateur Radio Messaging, alive and well in the 21st Century"; Ben Kuo, AI6YR, "How Social Media, the Internet, and Ham Radio saved the day after Hurricane Maria in Dominica"; and Stu Sheldon, AG6AG, "I just got my Amateur Radio License, Now what???"For those interested in getting started with Linux, SCaLE holds training sessions (e.g., Saturday and Sunday mornings). These sessions include an install-fest, encouraging participants to bring a machine and work one-on-one with SCaLE training proctors to help get Linux installed and operational. In the afternoon, a trainer from the Linux Foundation covers basic system administration skills. These classes are first come, first served — so if you're interested, come early to get a seat. Hardware requirements and other event related information is posted on the SCaLE web site.

As many past participants (and volunteers) can attest, SCaLE is a fun event! I'm sure that if you come, you'll enjoy yourself more than you might think; and who knows, you might even learn a thing or two in the process!

2018 SARA Western Conference

Palo Alto, California
March 23 – 25, 2018
www.radio-astronomy.org

The 2018 SARA Western Conference will be held at Stanford University in Palo Alto, California on Friday, Saturday and Sunday, March 23 – 25, 2018. The first day will include a visit to the Kavli Institute for Particle Physics and Cosmology (KIPAC) facilities at the Stanford Linear Accelerator Center (SLAC). The next two days' meetings will take place on the Stanford University campus and will include presentations by members and guest speakers. A board meeting for the Society will also be held during the conference.

Getting there: Fly into the San Jose or San Francisco airport and rent a car to drive to Palo Alto. It is also possible to use CALTRAIN to get from the San Jose or San Francisco airport to Palo Alto, but you would still need a car to get from the hotel to the meeting site at Stanford University.

Registration: Registration for the 2018 Western Conference is just $60.00 US. This includes snacks and lunch on Saturday and Sunday. Breakfast should be eaten at the hotel. Payment can be made through PayPal, **www.paypal.com** by sending payment to **treas@radio-astronomy.org**. Please include in comments that the payment is for the 2018 Western Conference. You may also mail a check payable to SARA Treasurer, c/o Bill Dean, 2946 Montclair Ave., Cincinnati, OH 45211. Please include an e-mail address so a confirmation can be sent to you when we receive your payment.

Hotel: Marriott Courtyard Palo Alto Los Altos, 4320 El Camino Real, Los Altos, CA 94022. Tel. (650) 941-9900. (Group Rate $139 per night plus taxes = $154.56 per night). Last day to book is March 2, 2018.

Additional Information: Additional details will be published online. Please contact conference coordinator David Westman if you have any questions or if you would like to help with the conference: **westernconf@radio-astronomy.org**.

The 2nd Annual Utah Digital Communications Conference

Sandy, Utah
March 28, 2018
utah-dcc.org

The 2nd Annual Utah Digital Communications Conference will be held March 24, 2018 at the Lake Community College Conference Center in Sandy Utah. The conference will be a fusion of Amateur Radio communications and Maker topics. Amateur Radio is the pioneer of digital modes. This conference will focus on the Amateur Radio hobby that surrounds utilizing digital modes. Current emerging topics such as digital modes for emergency communications and building your own components. If you have questions please email **UtahDCC@gmail.com**

Registration: Registration after February 24, 2018 is $20 per person. You can register using the EventBrite system. Check the website for instructions and other payment options.

2018 Southeastern VHF Conference

Valdosta, Georgia
April 26 – 29, 2018
svhfs.org/wp/

The 2018 Southeastern VHF Society Conference will be in Valdosta, Georgia, hosted by the Suwannee Amateur Radio Club and Down East Microwave Inc. The festivities will start on Thursday afternoon, April 26 and continue through Sunday morning, April 29. The main conference will be held in the Holiday Inn Hotel and Conference Center located only seconds from I-75 in Valdosta, Georgia.

Reservations: The Holiday Inn is just now completing its renovation and will provide a great site for our conference. The Southeastern VHF society has a guaranteed room rate of $89 for the weekend and surrounding days if you plan to stay for a short vacation. A block of rooms has also been reserved in the Super 8 at $69 per night. Super 8 shares the same parking area and is in walking distance of the actual Conference Center. Please see website for hotel reservation information.

As usual, the conference will offer presentations, antenna and equipment testing, along with a chance to get together with other Society members through the weekend.

We expect to conduct the Best Paper and Presentation competition, and will offer some great prizes, along with prizes at the Banquet. There will be a family program this year that will visit sites in Southern Georgia and Northern Florida.

Conference and Banquet pricing will be announced soon, along with the opening of registration and any other special events that may become available throughout the process. Check the website for details.

Call for Papers: Papers and presentations are solicited on both the technical and operational aspects of VHF, UHF and Microwave weak signal Amateur Radio. Some suggested areas of interest are: transmitters, receivers, transverters; RF power amplifiers, RF low noise preamplifiers; antennas; construction projects; test equipment and station accessories; station design and construction; contesting, roving, DXpeditions; EME, propagation (sporadic E, meteor scatter, troposphere ducting, etc.); digital modes, digital signal processing (DSP), software defined radio (SDR); amateur satellites and amateur television

In general, papers and presentations on non-weak signal related topics such as FM repeaters and packet will not be accepted but exceptions may be made if the topic is related to weak signal. For example, a paper or presentation on the use of FM simplex in contests or on the use of APRS to track rovers during contests would be considered.

All submissions for publication in the proceedings should be in Microsoft Word (.doc or .docx) formats. Submissions for presentation at the conference should be in Microsoft PowerPoint (.ppt or .pptx) format and delivered at the conference on a USB memory stick. Please understand that your Power Point Slide presentation will not be accepted to be published in the proceedings. Only meaningful text will be published in the proceedings not slides that need description for understanding.

The deadline for the submission of papers and presentations is **March11, 2018**. Please indicate when you submit your paper or presentation if you plan to attend the conference and present your paper in person, or if you are submitting solely for publication. Papers and presentations are being handled by Sandra Estevez, K4SME, and should be sent to: **conference papers@downeastmicrowave.com**.

Sandra may be contacted at the same e-mail address if you have any questions. Formatting instructions can be found on the website.

2018 Central States VHF Society Conference

Wichita, Kansas
July 26-29, 2018
www.2018.CSVHFS.org

Call for papers: Papers are being solicited for publishing in the *Proceedings of the 2018 Central States VHF Conference* on all weak-signal VHF and above Amateur Radio topics, including: antennas: including modeling, design, arrays, and control; test equipment: including homebrew, commercial, and measurement techniques and tips; construction of equipment such as transmitters, receivers, and transverters; operating, including contesting, roving, and DXpeditions; RF power amps, including single and multi-band vacuum tubes, solid-state, and TWTAs; propagation, including ducting, sporadic E, tropospheric, meteor scatter, etc.; Preamplifiers (low noise); digital modes, such as WSJT, JT65, FT8, JT6M, ISCAT, etc.; regulatory topics; moon bounce (EME); software-defined radio (SDR); and digital signal processing (DSP).

Topics such as FM, repeaters, packet radio, etc., are generally considered outside of the scope of papers being sought. However, there are always exceptions. If you have any questions about the suitability of a particular topic, contact **wa2voi@mninter.net**.

You do not need to attend the conference nor present your paper to have it published in the *Proceedings*.

Deadline for receipt of papers for inclusion in the Proceedings is **Tuesday, May 15, 2018.**

Complete information, including a style guide, can be found on the Central States VHF Society, Inc. website.

ARRL/TAPR Digital Communications Conference (37th)

Albuquerque, New Mexico,
September 14-16, 2018
www.tapr.org

The 37th Annual ARRL and TAPR Digital Communications Conference will be held September 14-16, 2018. in Albuquerque, New Mexico, at the Sheraton Albuquerque Airport Hotel. Rocky Mountain Ham Radio will be hosting the event.

The ARRL and TAPR Digital Communications Conference is an international forum for radio amateurs to meet, publish their work, and present new ideas and techniques. Presenters and attendees will have the opportunity to exchange ideas and learn about recent hardware and software advances, theories, experimental results, and practical applications.

Hotel and registration information will be available soon. Please check the website.

Call for Papers: Technical papers are solicited for presentation at the ARRL and TAPR Digital Communications Conference and publication in the Conference Proceedings. Annual conference proceedings are published by the ARRL. Presentation at the conference is not required for publication. Submission of papers are due by **July 31st, 2018** and should be submitted to: Maty Weinberg, ARRL, 225 Main St., Newington, CT 06111

Topics include, but are not limited to: Software Defined Radio (SDR), digital voice (D-Star, P25, WinDRM, FDMDV, DRMDV, G4GUO), digital satellite communications, Global Position System (GPS), precision timing, Automatic Packet Reporting System^{tm} (APRS), short messaging (a mode of APRS), Digital Signal Processing (DSP), HF digital modes, Internet interoperability with Amateur Radio networks, spread spectrum, IEEE 802.11 and other Part 15 license-exempt systems adaptable for Amateur Radio, using TCP/IP networking over Amateur Radio, mesh and peer to peer wireless networking, emergency and Homeland Defense backup digital communications, using Linux in Amateur Radio, updates on AX.25 and other wireless networking protocols, and topics that advanced the Amateur Radio art.

Ham Radio: Where Hands-On Lives On!

NEW! ARRL's Hands-On Radio Experiments

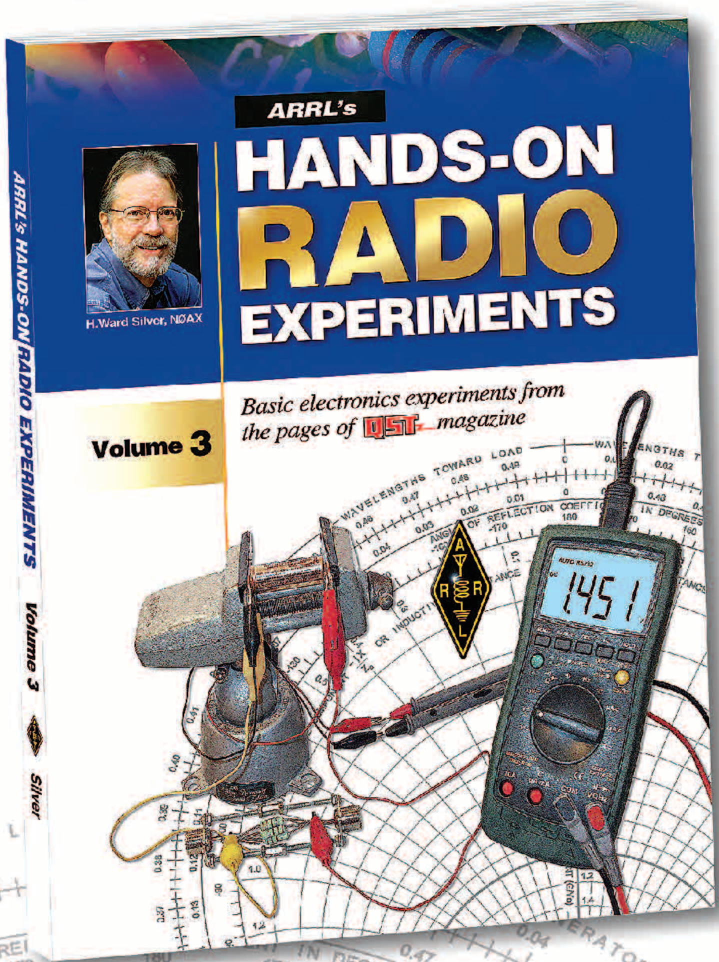

Volume 3

Lifelong learners will welcome Volume 3 of ***ARRL's Hands-On Radio Experiments***, assembled from the past four years (2013-2017) of *QST's* monthly "Hands-On Radio" column, written by Ward Silver, N0AX. Silver expertly leads you through 57 basic electronics experiments, designed to increase your understanding of radio fundamentals, components, circuits and design. As in the previous volumes, the experiments span an eclectic mix of topics:

- Electronic Circuits
- Antennas and Propagation
- Transmission Lines and Impedance Matching
- Electronic Fundamentals
- Electronic Components
- Tests and Test Equipment
- RF Techniques
- Practical Station Practices

Includes a complete **parts list** from all experiments in Volumes 1, 2 and 3!

ARRL's Hands-On Radio Experiments
Volume 3
ARRL Item No. 0796
Member Price! Only $19.95
(retail $22.95)

"As long as we keep putting our hands on radios, there will be new things to learn and techniques to try!"

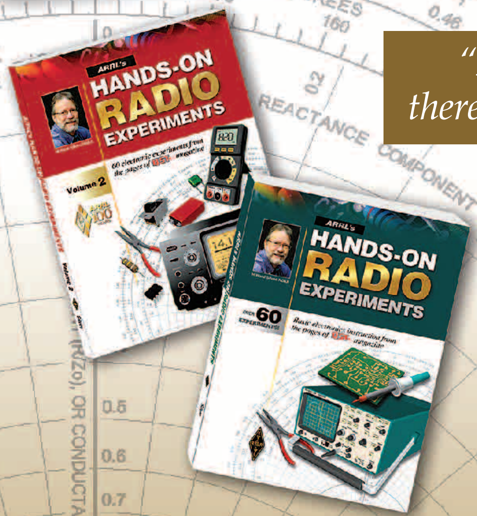

Collect the Entire Set! Also available:

ARRL's Hands-On Radio Experiments Volume 2
ARRL Item No. 3411
Member Price! Only $19.95

ARRL's Hands-On Radio Experiments
ARRL Item No. 1255
Member Price! Only $19.95

ARRL The national association for AMATEUR RADIO®

www.arrl.org/shop

Toll-Free US 888-277-5289,
or elsewhere +1-860-594-0355